Genome-wide identification of target genes of a mating-type α-domain transcription factor reveals functions beyond sexual development

Citation	Becker, K., Beer, C., Freitag, M., & Kück, U. (2015). Genome-wide identification of target genes of a mating-type α-domain transcription factor reveals functions beyond sexual development. Molecular Microbiology, 96(5), 1002-1022. doi:10.1111/mmi.12987
DOI	10.1111/mmi.12987
Publisher	John Wiley & Sons, Inc.
Version	Version of Record
Terms of Use	http://cdss.library.oregonstate.edu/sa-termsofuse

Molecular Microbiology (2015) 96(5), 1002–1022 ■
doi:10.1111/mmi.12987
First published online 28 March 2015

Genome-wide identification of target genes of a mating-type α-domain transcription factor reveals functions beyond sexual development

Kordula Becker,[1] Christina Beer,[1] Michael Freitag[2] and Ulrich Kück[1]*
[1]*Christian Doppler Laboratory for Fungal Biotechnology, Lehrstuhl für Allgemeine und Molekulare Botanik, Ruhr-Universität Bochum, Universitätsstr. 150, D-44780 Bochum, Germany.*
[2]*Department of Biochemistry and Biophysics, Oregon State University, Corvallis, Oregon 97331-7305, USA.*

Summary

Penicillium chrysogenum **is the main industrial producer of the β-lactam antibiotic penicillin, the most commonly used drug in the treatment of bacterial infections. Recently, a functional *MAT1-1* locus encoding the α-box transcription factor MAT1-1-1 was discovered to control sexual development in *P. chrysogenum*. As only little was known from any organism about the regulatory functions mediated by MAT1-1-1, we applied chromatin immunoprecipitation combined with next-generation sequencing (ChIP-seq) to gain new insights into the factors that influence MAT1-1-1 functions on a molecular level and its role in genome-wide transcriptional regulatory networks. Most importantly, our data provide evidence for mating-type transcription factor functions that reach far beyond their previously understood role in sexual development. These new roles include regulation of hyphal morphology, asexual development, as well as amino acid, iron, and secondary metabolism. Furthermore, *in vitro* DNA–protein binding studies and downstream analysis in yeast and *P. chrysogenum* enabled the identification of a MAT1-1-1 DNA-binding motif, which is highly conserved among euascomycetes. Our studies pave the way to a more general understanding of these master switches for development and metabolism in all fungi, and open up new options for optimization of fungal high production strains.**

Accepted 26 February, 2015. *For correspondence. E-mail ulrich.kueck@rub.de; Tel.: (+49) 23 4322 6212; Fax (+49) 23 4321 4184.

Introduction

Sexual propagation in euascomycetes is controlled by two alternative mating-type loci, namely *MAT1-1* and *MAT1-2*, which consist of dissimilar sequences occupying the same locus on the chromosome. These sequences are termed idiomorphs to indicate that they do not represent the alleles of a single gene (Metzenberg and Glass, 1990). A common feature specific to mating types from euascomycetes is the presence of a *MAT1-1-1* gene, defining the *MAT1-1* idiomorph and encoding an α-domain transcription factor (TF). The alternative idiomorph, *MAT1-2*, is characterized by the presence of a *MAT1-2-1* gene, encoding a TF carrying a high mobility group (HMG) domain (Turgeon and Yoder, 2000; Lee *et al.*, 2010).

While DNA-binding HMG-domain proteins are ubiquitous and well characterized, α-domain proteins have limited distribution and their evolutionary origin is still obscure (Martin *et al.*, 2010). In *Saccharomyces cerevisiae*, MATα1, one of two proteins encoded by the α-type mating locus, acts as a transcriptional co-activator and is involved in the regulation of mating-type-specific gene expression (Herskowitz, 1989). MATα1 binds cooperatively with the MADS-box TF Mcm1 to 26-bp P′Q promoter elements to activate the expression of α-specific genes (αsgs) (Bender and Sprague, 1987). Surprisingly, only a few direct target genes of mating-type TFs are known until today. For example, chromatin immunoprecipitation (ChIP)-chip analysis in *S. cerevisiae* identified five αsgs and six a-specific genes (asgs), which, with the exception of one αsg, were all involved directly in some aspect of mating, e.g. those encoding the mating pheromone α-factor and the a-pheromone receptor Ste3 (Galgoczy *et al.*, 2004). Similarly, microarray analysis in *Candida albicans* identified two αsgs and at least two asgs (Tsong *et al.*, 2003), and genome-wide ChIP analysis in *Lachancea kluyveri* identified a total of nine asgs, of which six were orthologs of asgs in either *C. albicans* or *S. cerevisiae* (Baker *et al.*, 2012). Against this background, it appears somehow contradictory that several microarray analyses demonstrated that *MAT* genes have a rather wide-ranging effect on fungal gene expression

(Pöggeler *et al*., 2006; Bidard *et al*., 2011; Wada *et al*., 2012; Böhm *et al*., 2013). Hence, further research is needed in order to distinguish between primary and secondary target genes of mating-type encoded TFs, and to provide a comprehensive understanding of mating-type controlled regulatory circuits on a genome-wide level.

As most research performed on characterizing mating-type locus-encoded TFs used yeasts as a model organism, little is known about mating-type protein function in euascomycetes. Lack of research on many euascomycetes, especially those of major medical and industrial importance, was fostered by the fact that these fungi have been considered to be asexual since no sexual propagation had been observed under laboratory conditions for a very long time (Dyer and O'Gorman, 2012; Kück and Böhm, 2013). Recent description of a hetherothallic sexual cycle in *P. chrysogenum* now makes the fungus a valuable object for the investigation of mating-type controlled transcriptional regulatory networks and fungal sexual reproduction in general. These mechanisms are of major importance, as the possibility to generate offspring with novel combinations of traits relevant to penicillin production provides promising starting points for industrial strain development purposes (Böhm *et al*., 2013).

Chromatin immunoprecipitation combined with next-generation sequencing analysis (ChIP-seq) is one of the most powerful tools for genome-wide profiling of DNA-binding proteins, which has greatly benefited from tremendous progress in next-generation sequencing technology (Smith *et al*., 2010; Magnúsdóttir *et al*., 2013; Myers *et al*., 2013). Today, ChIP-seq is an indispensable tool for studying gene regulation and epigenetic mechanisms at the genomic level (Park, 2009). Here, we present the first application of ChIP-seq for the functional characterization of a TF from *P. chrysogenum*, and, more importantly, the first genome-wide analysis focusing on unraveling the transcriptional regulatory network controlled by a mating-type locus-encoded TF.

While MAT1-1-1 has been described as a regulatory protein restricted to the orchestration of sexual reproduction (Debuchy *et al*., 2010), our data clearly expand this current view of MAT1-1-1 function beyond transcriptional regulation of sexual development alone. We provide strong evidence of new and additional roles for MAT1-1-1 in regulating asexual development and morphogenesis, as well as amino acid, iron, and secondary metabolism. Furthermore, our analyses, using bioinformatics, electrophoretic mobility shift assays (EMSAs), yeast one-hybrid (Y1H), and *DsRed* reporter gene assays in *P. chrysogenum*, led to the identification of a MAT1-1-1 DNA-binding motif that shows a high degree of conservation within euascomycetes.

Taken together, our data extend the general understanding of the biological functions of mating-type-encoded TFs and should thus open new avenues for the study of fungal sexual development. Finally, as we performed ChIP-seq experiments with a laboratory strain that has already undergone several rounds of mutagenesis to increase penicillin production (Nielsen, 1997), our results are applicable to fungal strains used for today's industrial production of pharmaceutically relevant secondary metabolites.

Results

Construction of MAT1-1-1 strains for ChIP-seq analysis

A P_{gpd}::*egfp*::*MAT1-1-1* fusion construct (pGFP-MAT1, Fig. S1A) was transformed into recipient P2niaD18 to generate strain MAT1-ChIP. P_{gpd} was used to obtain an elevated expression level of the *MAT1-1-1* gene, since expression of mating-type genes under control of their native promoter is known to be low. For example, RMAexpress (http://rmaexpress.bmbolstad.com) analysis of normalized raw data obtained from microarray analysis using *P. chrysogenum* strain P2niaD18 revealed relative *MAT1-1-1* expression levels of about 13.6% and 3.1% referred to actin (*Pc20g11630*) and myosin (*Pc21g00710*) expression levels, respectively (Fig. S1B) (Böhm *et al*., 2013). Furthermore, transcripts of mating-type genes were reported to be barely detectable by Northern hybridization in *Podospora anserina* as well as RNA-seq analysis in *Neurospora crassa* (Coppin and Debuchy, 2000; Wang *et al*., 2014).

Successful transformation was verified by polymerase chain reaction (PCR) and sodium dodecyl sulfate–polyacrylamide gel electrophoresis (SDS–PAGE)/Western blot analysis, confirming the presence of the epitope-tagged protein EGFP-MAT1-1-1 in crude protein extract from recombinant strains (Fig. S1C and D). Using fluorescence microscopy, the presence and nuclear localization of the fusion protein were verified prior to each ChIP experiment (Fig. S1E). Functionality of the fusion protein was further confirmed when pellet formation was investigated in shaking cultures (Fig. S1F). Overexpression of *MAT1-1-1* in the MAT1-ChIP strain resulted in the formation of significantly larger pellets (Ø 4–5 mm) when compared with P2niaD18 (Ø 1–2 mm), matching the phenotypic characteristics of a previously described *MAT1-1-1* overexpression strain (OE MAT1-1-1) (Böhm *et al*., 2013).

ChIP-seq analysis reveals a genome-wide binding profile of MAT1-1-1

We performed ChIP-seq experiments on three independent biological samples, namely 'shaking 1', 'shaking 2', and 'surface' (Table 1). In an effort to identify as many

Table 1. ChIP-seq design and results.

Sample	# Reads[a]	# Mapped[b]	% Mapped[c]	# Peaks FDR ≤ 0.001[d]	# Differential peaks[e]	# Total peaks[f]	Estimated fragment length[g]
shaking 1	44,608,426	27,190,663	60.9 %	7453	430	327	237
shaking 2	39,771,172	23,994,317	60.3 %	6523	379	276	226
surface	14,364,485	12,890,352	89.7 %	6324	218	102	212
shaking_input	16,952,199	15,380,186	90.7 %	–	–	–	–
surface_input	12,879,889	11,422,613	88.7 %	–	–	–	–

a. Total number of sequenced reads.
b. Total number of reads mapped to *P. chrysogenum* P2niaD18 genome (Specht *et al.*, 2014).
c. Fraction of tags found in peaks versus genomic background determined by HOMER (Heinz *et al.*, 2010).
d. Number of peaks passing FDR ≤ 0.001 threshold.
e. Number of peak regions showing at least fourfold enrichment in ChIP-sample compared to input.
f. Total number of peak regions after local background filtering and clonal filtering.
g. Estimated fragment length used for sequencing, determined from tag auto correlation analysis.

MAT1-1-1 binding sites as possible, independent of physiological culture conditions, two samples were derived from shaking cultures and one was obtained from a surface-grown culture. Input-DNA from shaking ('shaking_input') and surface cultures ('surface_input') was sequenced as a control. Only regions meeting the following criteria were considered as specific peak regions: (1) at least fourfold enrichment in ChIP-DNA versus input-DNA, (2) a false discovery rate (FDR) threshold ≤ 0.001, and (3) a Poisson *p*-value ≤ 1.00e–04. Intersection of our datasets identified 243 sites that were specifically bound by MAT1-1-1 in at least two independent biological replicates, thus meeting the standards set by the ENCODE and modENCODE consortia (Landt *et al.*, 2012) (Dataset S1, Fig. 1A).

Starting from ChIP-seq datasets, we classified peaks according to their genomic location with regard to neighboring coding sequences. Seventy-nine percent (193/243) of peaks were exclusively located within intergenic regions and 21% (50/243) showed intragenic localization (Fig. 1B). Of 193 peaks showing intergenic localization, 21 were positioned within the 3′ region of both neighboring open reading frames, and 90 showed 5′ localization to only one adjacent gene. Eighty-two peak regions were, however, positioned within divergent promoters, resulting in a total of 254 genes that may be directly controlled by MAT1-1-1. Comparison to expression data obtained from previous microarray analyses (Böhm *et al.*, 2013) confirmed changes in expression profiles by at least twofold in a Δ*MAT1-1-1* strain compared with P2niaD18 for 29.9%

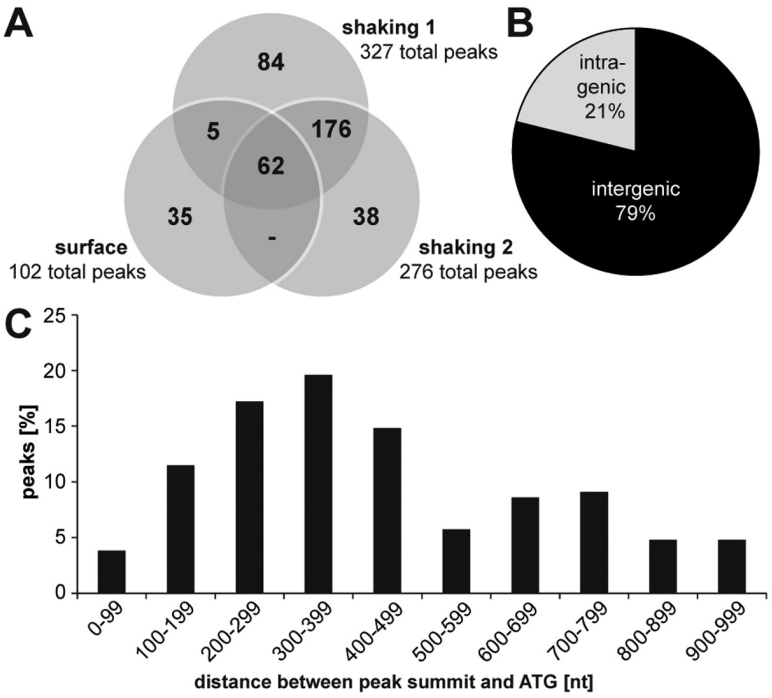

Fig. 1. Genome-wide distribution of MAT1-1-1 binding regions.
A. Venn-diagram showing intersection between MAT1-1-1 'shaking 1', 'shaking 2', and 'surface' datasets. Only peaks within a maximum distance of 100 nt were regarded as overlapping.
B. Distribution of ChIP-enriched regions overlapping or positioned within intragenic regions vs. ChIP-enriched regions that were exclusively located within intergenic regions (based on peak regions present in at least two independent datasets).
C. Distance between MAT1-1-1 ChIP-seq peak summits and ATG of neighboring genes positioned in 5′–3′ orientation with regard to the corresponding peak region (based on peak regions present in at least two independent datasets).

(76/254) of these genes. Analysis of the distance between peak summits and the predicted translation start sites (nearest ATG in good initiation context) revealed an average distance of 200–500 nt (Fig. 1C). Approximately 50% of all analyzed genes fit this pattern.

Categorization of putative MAT1-1-1 target genes

Gene ontology (GO) analysis of proteins encoded by the 254 putative MAT1-1-1 target genes revealed a significant ($p \leq 0.05$) overrepresentation of the following categories: (1) metabolism, including proteins related to amino acid and secondary metabolism, (2) energy, (20) cellular transport, transport facilities, and transport routes, (32) cell rescue, defense, and virulence, (34) interaction with the environment, including proteins involved in cellular sensing and response to external stimuli (e.g. pheromone response) (Fig. S2). Besides expected putative MAT1-1-1 target genes that could be directly assigned to sexual development, e.g. *ppg1* (*Pc14g01160*), the homolog of *S. cerevisiae MFα1/2*, encoding the α-factor pheromone, and *pre1* (*Pc22g15650*), the homolog of the *S. cerevisiae* a-factor receptor encoding gene *STE3* (Galgoczy *et al.*, 2004), ChIP-seq analysis identified many new putative MAT1-1-1 target genes that had never been linked to mating-type-encoded TFs before. Table 2 provides a detailed summary of selected MAT1-1-1 target genes arranged according to the description and proposed function of encoded proteins, as obtained from blastp analysis and literature. All genes listed are positioned in 5′–3′ orientation with regard to neighboring MAT1-1-1 peak regions. Corresponding peak values, expression profiles of each gene in a *MAT1-1-1* deletion strain compared with wild type P2niaD18 and occurrence of the MAT1.1 motif (to be described later) are given. For reasons of clarity and comprehensibility, the categories mentioned here do not necessarily correspond directly to categories used in GO analysis.

Validation of MAT1-1-1 targets

To validate MAT1-1-1 DNA-binding regions identified by our ChIP-seq approach, we performed ChIP-PCR analysis (Fig. 2A). Five representative MAT1-1-1 target regions were analyzed for MAT1-1-1-specific enrichment in ChIP-DNA compared to input-DNA, obtained from shaking cultures. Target regions were selected according to the following two key criteria: (1) they either possessed a statistically highly significant peak value (*Pc20g00090*) or (2) proteins encoded by adjacent genes were known to be involved in regulation of sexual reproduction in yeast (*pre1*, *kex1*, *kex2*, *ppg1*). Enrichment was calculated as the ratio of the region of interest to a control region showing no MAT1-1-1-specific enrichment in ChIP-DNA relative to this ratio in the input-DNA sample. An additional control region (NC) is shown as a negative control. ChIP-PCR results showed significant overlap with the corresponding peak values obtained from bioinformatics analysis, confirming specific enrichment of all tested target regions in ChIP-DNA vs. input-DNA, and validating peak values as a convincing parameter for estimation of MAT1-1-1 binding affinity to target regions identified in ChIP-seq analyses.

Next, quantitative real time (qRT)-PCR analyses were performed to validate MAT1-1-1 target genes next to the peak regions mentioned earlier as well as a selection of additional, non-mating-related target genes, covering all functional protein categories mentioned in Table 2. Compared with wild type P2niaD18, expression levels of putative target genes were examined in shaking cultures of a *MAT1-1-1* deletion strain (ΔMAT1) or *MAT1-1-1* overexpression strain (MAT1-ChIP), grown under the same conditions as for ChIP-seq sample preparation. A total of four mating- and 13 non-mating-related genes were selected for our investigation. Compared with P2niaD18, overexpression of *MAT1-1-1* in the MAT1-ChIP strain led to significant changes in expression levels of 3 genes related to some aspect of sexual reproduction, namely *pre1*, *kex1*, and *ppg1*, as well as seven non-mating-related genes, namely *Pc20g00090*, *dewA*, *atf21*, *Pc19g00140*, *sidD*, *Pc22g27040*, and *Pc22g22160* (Fig. 2B and Fig. S3A). Similar results were obtained when ΔMAT1 expression levels were measured. It is remarkable that all these genes are located in 5′–3′ orientation relative to the adjacent peaks, thus, validating our criteria applied for identification of putative MAT1-1-1 target genes based on data obtained from ChIP-seq analysis.

De novo *prediction of a MAT1-1-1 DNA-binding motif*

To gain further insight into MAT1-1-1 DNA-binding properties, *de novo* motif prediction based on MAT1-1-1-binding regions, identified in our ChIP-seq analysis, was performed. We used MEME to identify conserved motifs, and therefore the most likely binding site of MAT1-1-1 in *P. chrysogenum*. MEME analysis, based on 62 MAT1-1-1 binding regions, present in three independent ChIP-seq experiments, identified one highly significant motif, designated MAT1.1, which showed a high degree of central enrichment across MAT1-1-1 peak regions in CentriMo analysis (Fig. 3). Furthermore, FIMO analysis confirmed the presence of at least one copy of MAT1.1 within 202 of 243 (83.1%; p-value ≤ 0.01) MAT1-1-1 peak regions, indicating that the vast majority but not all MAT1-1-1 target sites are bound at this motif.

Comparison of MAT1.1 to known binding motifs present in the JASPAR CORE (2014) databases for fungi and vertebrates revealed strong similarity to the binding sites

Table 2. Selected MAT1-1-1 target regions obtained from ChIP-seq analysis.

Identifier	Description[a]	Proposed function	Peak value[b]	Microarray[c] 36 h	Microarray[c] 96 h	MAT1.1[d] $p \leq 0.001$	MAT1.1[d] $p \leq 0.01$
Sexual development							
Pc22g18600[e]	serine carboxypeptidase Kex1	Homolog of *S. cerevisiae* α-pheromone processing endoproteases KEX1 (Dmochowska *et al.*, 1987)	4540	–0.14	–1.07	3	6
Pc22g15650[e]	a-pheromone receptor Pre1	Homolog of the *S. cerevisiae* a-factor receptor STE3 (Galgoczy *et al.*, 2004)	3869	–0.11	–0.52	2	6
Pc22g02910[e]	pheromone-processing endoprotease Kex2	Homolog of *S. cerevisiae* α-pheromone processing endoprotease KEX2 (Julius *et al.*, 1984)	1396	0.42	0.02	2	3
Pc20g00540	cyclin-dependent protein kinase Bur1	Protein required for a G-α subunit-mediated adaptive pheromone-response in *S. cerevisiae* (Irie *et al.*, 1991)	861	0.23	–0.32	2	6
Pc14g01160[e]	mating α-pheromone Ppg1	Homolog of *S. cerevisiae* α-factor pheromone MFα1 (Galgoczy *et al.*, 2004)	663	0.30	–0.46	2	5
Pc12g15890	cAMP-independent regulatory protein Pac2	cAMP-independent regulatory protein modulating onset of sexual development in *Schizosaccharomyces pombe* and *Magnaporthe oryzae* (Kunitomo *et al.*, 1995; Chen *et al.*, 2014)	444	1.01	–0.04	0	0
Morphogenesis and asexual development							
Pc21g04930	trehalose-6-phosphate synthase subunit 3	Involved in biosynthesis of trehalose, a compound necessary for long-term viability of fungal spores (Elbein *et al.*, 2003)	747	–0.36	–0.18	0	1
Pc18g03940[e]	14-3-3 family protein ArtA	14-3-3 family protein involved in regulation of polarization of germinating conidiospores in *Aspergillus nidulans* (Kraus *et al.*, 2002)	724	0.13	0.07	0	1
Pc16g06690[e]	spore wall fungal hydrophobin DewA	Spore wall fungal hydrophobin responsible for hydrophobicity of conidiospores in *A. nidulans* (Stringer and Timberlake, 1995; Grünbacher *et al.*, 2014)	640	–3.87	0.05	0	4
Pc06g01300	thioredoxin TrxA	Involved in regulation of growth and formation of reproductive structures, e.g. conidiophores and cleistothecia, in *A. nidulans* (Thön *et al.*, 2007)	584	–3.91	0.41	1	4
Pc12g15180	chitin biosynthesis protein	Involved in biosynthesis of chitin, an essential component of the cell walls and septa, necessary for polarized growth, septa formation during hyphal growth, and conidia development (Fukuda *et al.*, 2009)	556	–1.37	0.11	0	1
Pc21g20900	cell morphogenesis protein PAG1	Cell morphogenesis protein, related to polarized morphogenesis and proliferation in *S. cerevisiae* (Du and Novick, 2002; Nelson *et al.*, 2003)	387	0.66	0.08	0	0
Pc22g26820[e]	bZIP TF Atf21	bZIP TF and repressor of sexual development in *A. nidulans* (Lara-Rojas *et al.*, 2011); activating TF/cAMP-response-element-binding protein, central role in maintaining cellular homeostasis and production of spores in *S. pombe* (Morita *et al.*, 2011)	324	2.00	0.74	1	2
Pc21g09870	related to integral membrane protein Pth11	Functions at the cell cortex as an upstream effector of appressorium differentiation in response to surface cues in *M. grisea* (DeZwaan *et al.*, 1999)	155	–1.29	0.56	0	4
Pc19g00140[e]	trehalose-6-phosphate synthase subunit	Involved in biosynthesis of trehalose, a compound necessary for long-term viability of fungal spores (Elbein *et al.*, 2003)	106	1.70	0.17	0	3
Amino acid and secondary metabolism							
Pc18g02620	cyanide hydratase/nitrilase	Likely to be involved in the cyanoamino acid metabolism	1712	–4.35	–0.40	0	2
Pc12g00820	MFS multidrug transporter Tpo1	Controls spermidine and spermine concentrations and mediates induction of antioxidant proteins, including Hsp70, Hsp90, Hsp104 and Sod1 in *S. cerevisiae* (Krüger *et al.*, 2013)	787	–0.85	0.37	2	6
Pc16g11470	ABC multidrug transporter AtrF	Overexpression correlates with itraconazole resistance in *A. fumigatus* (Slaven *et al.*, 2002)	690	1.25	1.06	0	0
Pc22g18630[e]	homocysteine S-methyltransferase	Catalyzes the chemical reaction of L-homocysteine to L-methionine [KEGG database]	645	0.59	–0.08	1	4
Pc12g02630	carbon catabolite repression protein CreD		623	–1.39	0.13	0	1
Pc16g06630	MFS multidrug transporter		597	–2.44	0.97	0	4
Pc20g03900	MFS multidrug transporter		525	–0.88	0.22	0	4
Pc22g06500	amino acid transporter		367	0.54	1.04	0	2
Iron metabolism							
Pc22g20410	siderophore biosynthesis lipase		1138	0.50	1.38	0	4
Pc22g20400[e]	non-ribosomal peptide synthetase SidD	Non-ribosomal siderophore peptide synthetase important for biosynthesis of intracellular siderophore triacetylfusarinine C (TAFC) (Schrettl *et al.*, 2007)	1138	0.46	0.31	0	4
Pc21g08020[e]	iron transporter multicopper oxidase FetC	Ferrooxidoreductase involved in reductive iron assimilation in *A. fumigatus* (Schrettl *et al.*, 2004)	882	–1.04	0.95	0	1
Pc21g08030[e]	high-affinity iron ion transporter FtrA	High-affinity iron permease that mediates uptake of $Fe2+$ during reductive iron acquisition in *A. fumigatus* (Schrettl *et al.*, 2004; Schrettl and Haas, 2011)	882	–1.18	1.57	0	1
Pc21g13060	ferric reductase transmembrane component		834	–0.08	–0.15	1	2
Pc13g11520	siderophore biosynthesis family protein		624	–0.19	1.81	0	1
Pc22g02380	MFS siderophore iron transporter		461	0.40	–0.36	0	0
Transcription factors							
Pc18g00880[e]	bZIP TF MeaB	bZIP TF involved in regulation of expression of nitrogen-dependent genes (Wong *et al.*, 2007; Schönig *et al.*, 2008)	1064	0.84	–0.03	2	3
Pc22g22160[e]	F-box domain protein		859	–2.35	0.16	2	4
Pc12g03120[e]	transcription factor Sin3	Master transcriptional scaffold protein and co-repressor that regulates cellular proliferation, differentiation, apoptosis, and cell cycle regulation in yeast as well as higher eukaryotes (Grzenda *et al.*, 2009)	616	0.33	–0.26	1	5
Pc20g05880	HLH TF		594	–1.95	–0.11	0	0
Pc18g01520	transcription initiation protein IIB		511	0.20	–0.11	1	3
Pc24g00540	C6 zinc finger domain protein		413	–2.89	1.16	1	2
Pc21g01450	TFIIIC transcription initiation factor complex subunit		393	0.47	–0.22	2	7
Pc22g27040[e]	C_2H_2 zinc finger domain protein		369	1.25	3.02	1	1

a. As obtained from blastp analysis (http://www.ncbi.nlm.nih.gov).
b. Statistical peak value = average tag count found at peak normalized to 10 Mio. total mapped tags.
c. Microarray data showing expressional changes in ΔMAT1 compared with wild type after 36 and 96 h of cultivation (Böhm *et al.*, 2013).
d. Number of MAT1.1 occurrences within peak region, *p*-value ≤ 0.001/0.01.
e. Verified using EMSA.

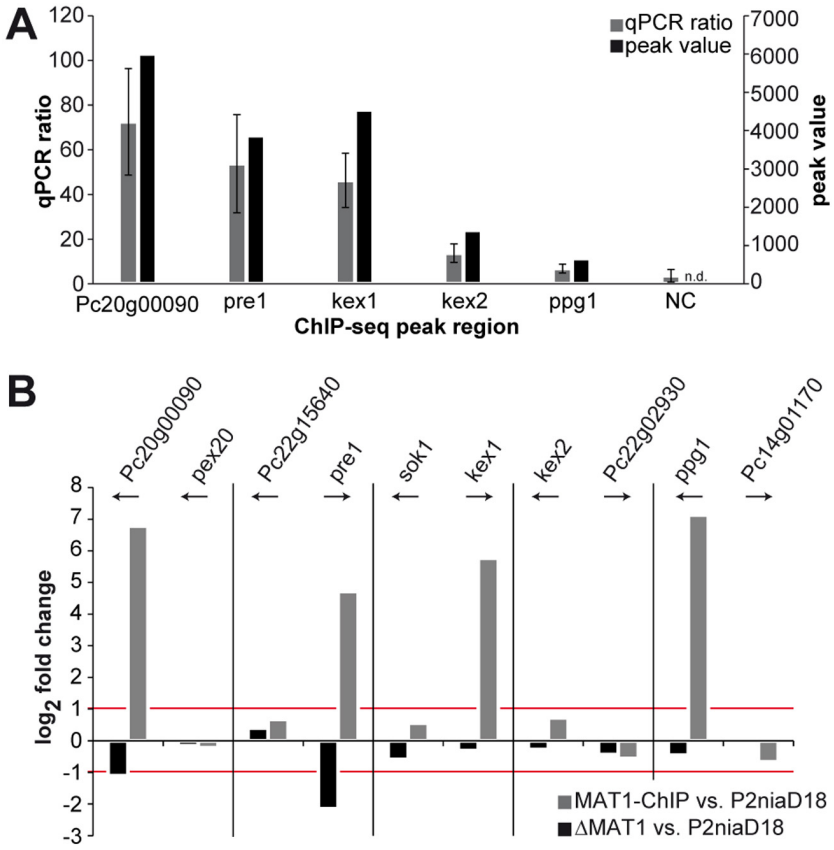

Fig. 2. Verification of MAT1-1-1 ChIP-seq data.
A. ChIP-PCR analysis was performed to verify enrichment of selected MAT1-1-1 binding regions in ChIP-DNA compared with input-DNA. Enrichment was calculated as the ratio of the region of interest to a control region showing no MAT1-1-1-specific enrichment in ChIP-DNA, relative to this ratio in the input-DNA sample. A region showing no MAT1-1-1-specific enrichment in ChIP-seq analysis is shown as a control (NC). Each qPCR ratio (gray bars) is shown in comparison to the corresponding peak value generated during bioinformatics analysis of ChIP-seq data (black bars). Values for qPCRs are the mean score of three biological replicates; average ± standard deviations are indicated. Tested peak regions are named according to neighboring genes (see *Dataset S1*).
B. Analysis of relative $\log_2$ fold gene expression ratios in a *MAT1-1-1* overexpression strain (MAT1-ChIP; gray bars) or *MAT1-1-1* deletion strain (ΔMAT1; black bars) compared with wild type strain P2niaD18 led to the identification of MAT1-1-1 specific target genes. Values are the mean score of three biological replicates. Tested genes represent pairs of genes positioned upstream and downstream of MAT1-1-1 target regions identified in ChIP-seq analysis (see *Dataset S1*). Directions of open reading frames are indicated by arrows.

of the *S. cerevisiae* mating-type protein MATa1 (Haber, 2012) and Mcm1, a TF involved in cell-type-specific transcription and pheromone response in yeast (Mead *et al.*, 2002) (Fig. S4). Furthermore, MAT1.1 showed similarity to DNA-binding motifs for Yhp1, a homeobox transcriptional repressor known to bind Mcm1 (Pramila *et al.*, 2002), and Hcm1, a forkhead TF regulating expression of genes involved in chromosome segregation, spindle pole dynamics and budding (Pramila *et al.*, 2006). Comparison to motifs known from vertebrates revealed strong similarity to the binding sites of Sox9, a SRY-related HMG-box protein, regulating the development of the skeleton and the reproductive system (Mertin *et al.*, 1999), Nkx2-5, a homeobox TF involved in the regulation of heart formation and development (Chen and Schwartz, 1995), as well as Sox17 and Sox2, SRY-related HMG-box proteins involved in the regulation of embryonic development and cell fate (Kanai *et al.*, 1996; Maruyama *et al.*, 2005).

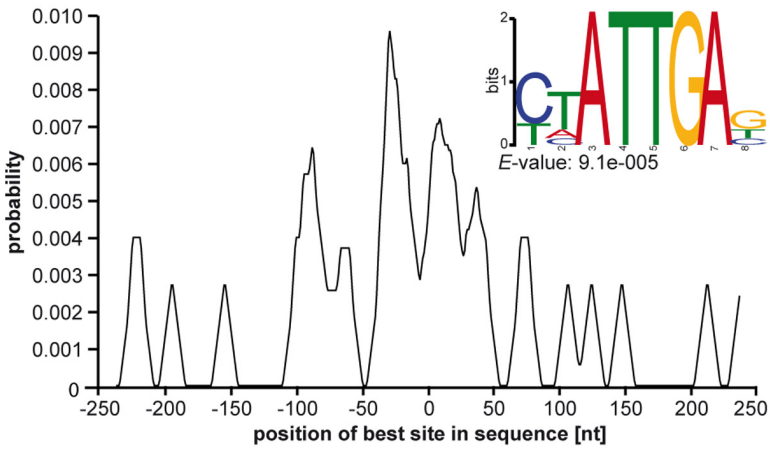

Fig. 3. *De novo* prediction of a MAT1-1-1 DNA-binding motif. The central 100 nt region of 62 MAT1-1-1 specific peak regions identified in three independent ChIP-seq experiments was submitted to MEME for identification of enriched motifs. Only the most significant putative DNA-binding motif ('MAT1.1') is shown. The size of each letter is proportional to the frequency of each nucleotide at this position within the consensus sequence. CentriMo analysis, using MAT1.1 as an input, revealed central enrichment of the motif within a 500 nt range around MAT1-1-1 binding regions used for motif prediction.

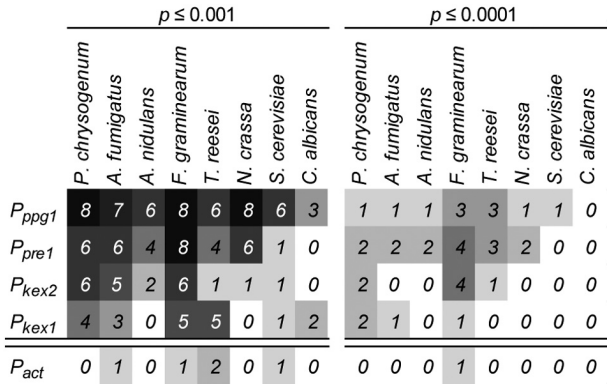

Fig. 4. Conservation of the MAT1.1 binding motif within ascomycetes. The 1000 nt upstream region of *ppg1*, *pre1*, *kex2*, and *kex1* from selected ascomycetes was screened for occurrences of MAT1.1 using FIMO. The 1000 nt upstream region of the actin gene *act* was used as a negative control. Total numbers of detected MAT1.1 copies within input sequences meeting a statistical threshold of $p \leq 0.001$ and $p \leq 0.0001$, respectively, are given. Locus tags according to NCBI database (http://www.ncbi.nlm.nih.gov/) are: *ppg1:* Pc14g01160, AFUA_6G06360, AN5791.2, CaO19.11961*, FG05061.1, NCU02500.1, YPL187W, TRIREDRAFT_104292; *pre1*: Pc22g15650, AFUA_5G07880, AN7743.2, CaO19.2492*, FG07270.1, NCU00138, YKL178C*, TRIREDRAFT_57526; *kex2*: Pc22g02910, AFUA_4G12970, AN3583.2, CaO19.12219, FG09156.1, NCU03219, YNL238W*, TRIREDRAFT_123561*; *kex1*: Pc22g18600, AFUA_1G08940, AN1384.2, CaO19.7020*, FG10145.1, NCU04316, YGL203C, TRIREDRAFT_74517; *act*: Pc20g11600, AFUA_6G04740, AN6542.2, CaO19.5007, FG07335.1, NCU04173, YFL039C*, TRIREDRAFT_77541. Asterisks are sequences shorter than 1000 nt.

The MAT1.1 binding motif shows conservation within euascomycetes

To address the question whether the predicted MAT1-1-1 DNA-binding consensus sequence MAT1.1 is conserved among ascomycetes, we performed FIMO analysis. For this purpose, the 1000 nt upstream region of *ppg1*, *pre1*, *kex2*, and *kex1* from *P. chrysogenum* and the corresponding homologs from *A. fumigatus*, *A. nidulans*, *C. albicans*, *Fusarium graminearum*, *N. crassa*, *S. cerevisiae*, and *Trichoderma reesei* were screened for occurrences of MAT1.1. The corresponding 1000 nt upstream sequences of the actin gene (*act*) were used as a negative control (Fig. 4). A high degree of conservation of MAT1.1 within the tested promoter regions of euascomycetes became obvious, whereas significant deviations were recognized when compared with hemiascomycetes. For example, applying a statistical threshold of $p \leq 0.0001$, occurrences of MAT1.1 were detected in seven out of eight *ppg1* (no occurrence in *C. albicans*) and six out of eight *pre1* (no occurrence in *S. cerevisiae* and *C. albicans*) upstream sequences. These observations were further confirmed when sequence alignments of the protein sequences of MAT1-1-1 DNA-binding domains revealed a significantly higher degree of conservation within the MAT_alpha1 domain (pfam04769), especially the region spanning the MATA_HMG-box (cd01389), of euascomycetes compared to hemiascomycetes, in particular, *C. albicans* (Fig. S5).

MAT1-1-1 binds in vitro *to MAT1.1*

Since our motif analysis suggested that MAT1-1-1 associates with DNA via the predicted DNA-binding consensus sequence CTATTGAG (MAT1.1), EMSAs were performed to test direct binding between DNA and protein. For this purpose, a GST-MAT1-1-1 fusion protein was purified from *Escherichia coli* BL21 (DE3) and the quality of the isolated protein was verified by SDS–PAGE/Western blot analysis using an antibody to GST (Fig. S6). The promoter regions of mating-related genes *pre1*, *kex1*, *kex2*, and *ppg1*, as well as 13 non-mating-related genes (marked in Table 2), which were bound by MAT1-1-1 in ChIP-seq analysis, were used to design oligonucleotide probes covering a region with at least one copy of MAT1.1 (Fig. 5A, Table S3).

All oligonucleotides harboring a complete, central copy of MAT1.1 were bound by GST-MAT1-1-1 (e.g. mating-related Pre1-2, Kex1-2, Kex2-2, Ppg1-2, and non-mating-related Pc20g00090-2, Pc22g27040-1, ArtA-1, DewA-1/-2, FetC/FtrA-1, and SidD-1), whereas probes lacking MAT1.1 (e.g. Pc20g00090-3, Pre1-3, Kex1-1) showed no binding (Fig. 5B and S3B). Only weak binding or no binding between DNA and protein was observed when MAT1.1 was positioned at the very end of the oligonucleotide or contained obvious deviations from the predicted consensus sequence (e.g. Kex1-3, Kex2-1, Ppg1-1, TrxA-1, and Pc16g06630-1). GST alone showed no binding to oligonucleotide Ppg1-2, confirming that the observed formation of protein–DNA complexes is mediated by MAT1-1-1, and not by the tag.

Fig. 5. Electrophoretic mobility shift assays (EMSAs) confirm MAT1-1-1-binding to ChIP-enriched genomic regions.
A. Zoomed ChIP-seq profiles of selected MAT1-1-1 ChIP-enriched regions. Positions and sequences of oligonucleotides used for shift analysis are indicated. Occurrences of the predicted MAT1-1-1 DNA-binding motif MAT1.1 are marked in red. Single nucleotides that do not fit the predicted consensus sequence are indicated in small letters. Maximum read counts at the summit of ChIP-seq peaks are indicated at the left. ORFs next to MAT1-1-1 ChIP-seq peak regions are marked by black boxes; arrowheads indicate 5′–3′ orientation.
B. EMSAs were performed using radiolabeled double-stranded oligonucleotide probes covering the central region of selected MAT1-1-1 target regions, identified in ChIP-seq analysis. Addition of GST-MAT1-1-1 protein is marked by (+), samples without protein are marked by (–). Positions of free probe (*) and protein–DNA complexes (→) are indicated.

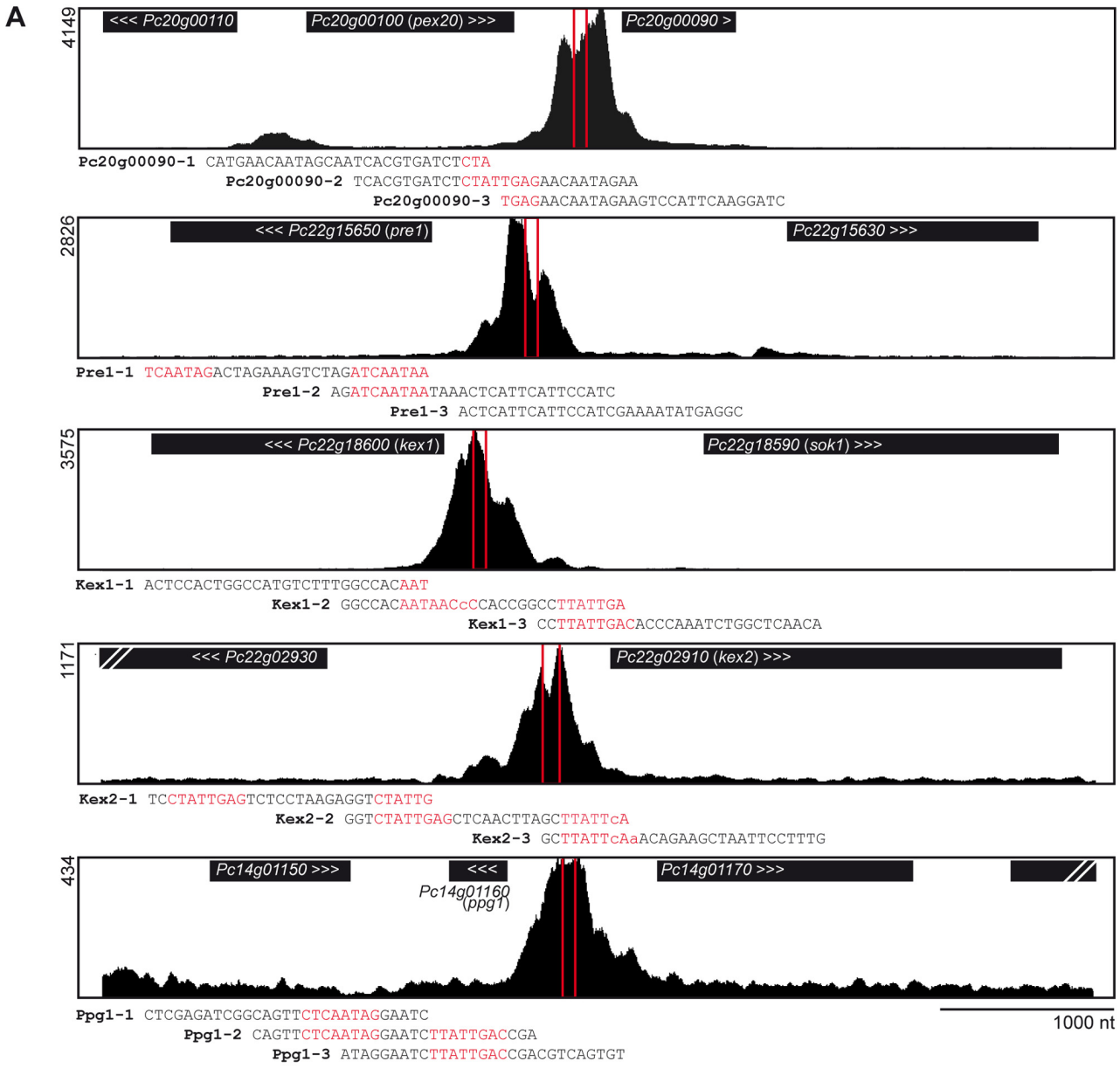

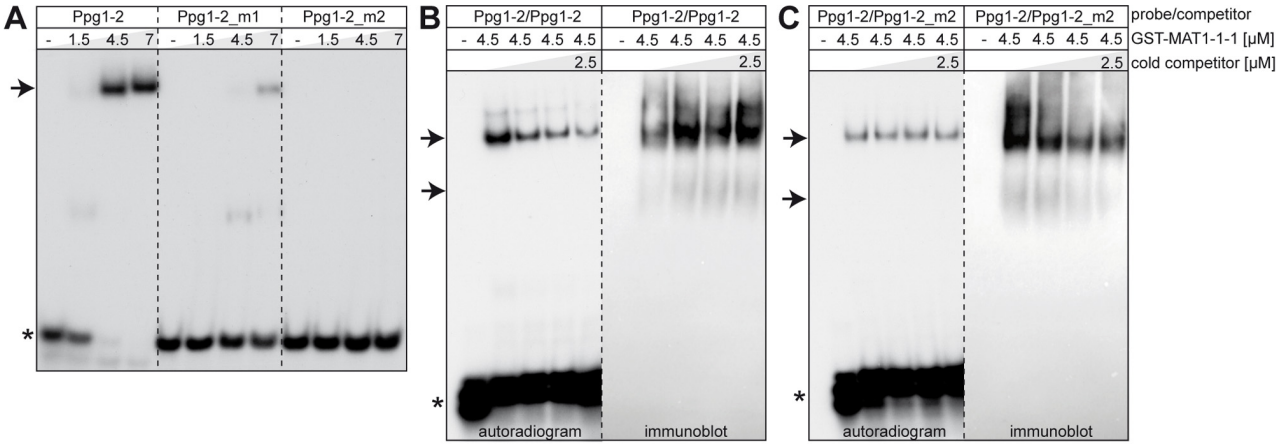

Fig. 6. Single-bp substitutions and Shift–Western analyses confirm specificity of MAT1-1-1 DNA-binding.
A. GST-MAT1-1-1 shows strong binding to a 30 nt double-stranded oligonucleotide derived from the *ppg1* promoter sequence (Ppg1-2), carrying two copies of the predicted MAT1-1-1 DNA-binding motif MAT1.1. A single A→G/T→C substitution at position 3 within one of two motif sequences (Ppg1-2_m1) results in a diminished formation of protein–DNA complexes. Complex formation is completely suppressed when both consensus sequences are mutated (Ppg1-2_m2).
B. Competition with increasing amounts of unlabeled Ppg1-2 oligonucleotide decreased the level of MAT1-1-1 binding to the labeled probe, leading to an attenuation of the shift band and accumulation of free labeled probe in shift experiments (autoradiogram, left panel). Western blotting and immunodetection (Shift–Western analysis), using an antibody to GST, showed an increase in complex signal strength when competing with unlabeled Ppg1-2 probe (GST-immunoblot, right panel).
C. Unlabeled Ppg1-2_m2 oligonucleotide did not compete for binding to MAT1-1-1 with labeled Ppg1-2, leading to a steady signal for protein–DNA complexes in shift experiments (autoradiogram, left panel) and a decrease in signal intensity in Shift–Western analysis (GST-immunoblot, right panel). The amount of protein used for shift analyses is indicated on top of each lane (1 µg of GST-MAT1-1-1 equals a molar concentration of 0.76 µM). Positions of free probe (*) and protein–DNA complexes (→) are indicated.

Specificity of MAT1-1-1 binding to MAT1.1 was further verified using mutated Ppg1-2 oligonucleotides. A single A → G or T → C substitution at position three of one of two copies of MAT1.1 present in oligonucleotide Ppg1-2_m1 led to a drastic reduction of protein–DNA complex formation, whereas mutation of both motifs (Ppg1-2_m2) totally abolished complex formation (Fig. 6A). Furthermore, competition assays using Ppg1-2 as a probe and unlabeled Ppg1-2 oligonucleotide as a competitor showed that the level of MAT1-1-1 binding to the labeled probe is diminished by addition of increasing amounts of the unlabeled competitor. In the corresponding autoradiogram, an attenuation of the shift band and accumulation of free labeled probe became visible (Fig. 6B; left panel). In contrast, Western blotting of the shift gel and immunodetection using an antibody to GST clearly showed an increase in complex signal strength when competing with unlabeled Ppg1-2 probe (Fig. 6B; right panel). Both, EMSA and Shift–Western analyses, confirmed the specificity of MAT1-1-1 binding to the Ppg1-2 oligonucleotide since addition of unlabeled DNA minimized binding of MAT1-1-1 to the radiolabeled probe, while overall complex formation was maximized. As expected, unlabeled Ppg1-2_m2 did not compete for binding to MAT1-1-1 with labeled Ppg1-2, leading to a steady protein–DNA complex signal in shift analysis and a decrease in signal intensity in Shift–Western analysis due to interference in overall complex formation as a result of a great excess of unbound competitor DNA (Fig. 6C).

MAT1-1-1 binding to MAT1.1 activates reporter gene expression in an ex vivo *yeast one-hybrid (Y1H) assay*

As biochemical assays confirmed MAT1-1-1 binding to the newly identified MAT1-1-1 DNA-binding motif MAT1.1 *in vitro*, yeast one-hybrid (Y1H) reporter gene assays were performed to validate binding *ex vitro*. Triple repeats of oligonucleotides Kex1-2 and Ppg1-2, as well as Ppg1-2_m1 and Ppg1-2_m2 in the promoter of the *lacZ* or *HIS3* reporter gene, were used as preys for MAT1-1-1. As bait, we used vector pMAT1-AD, containing the *MAT1-1-1* cDNA sequence and the activation domain of yeast Gal4 TF. Both prey and bait vectors were integrated into yeast a- and α-strains. Diploid strains, generated by mating and carrying one of the prey and the bait vector, were identified by growth on selective media lacking uracil and leucine. Furthermore, *HIS3* reporter gene activity, indicating MAT1-1-1 binding to the respective prey sequence, was analyzed on selective media lacking uracil, leucine, and histidine, but containing increasing amounts of 3-AT. In addition, qualitative and quantitative β-galactosidase assays were performed to measure *lacZ* reporter gene activity, thereby enabling evaluation of protein–DNA interactions based on two independent reporter gene systems.

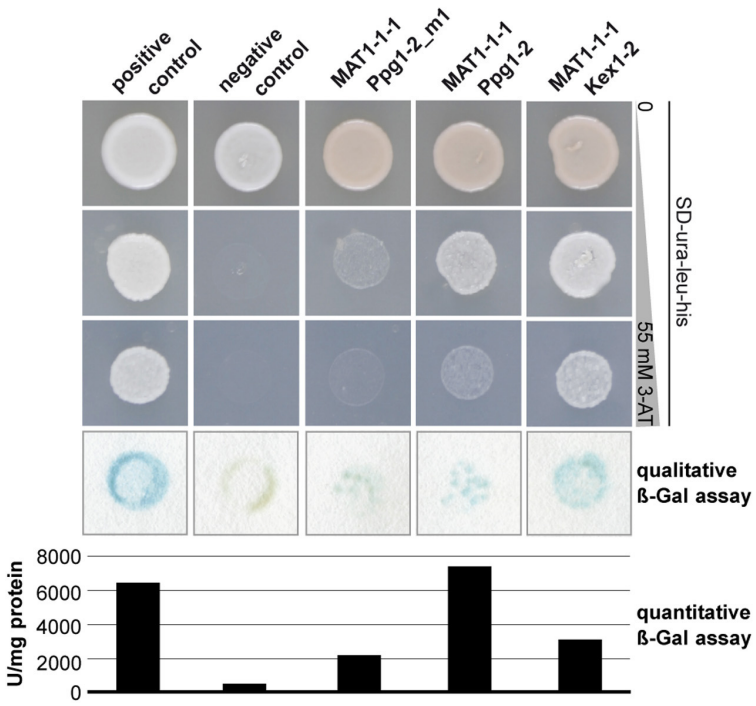

Fig. 7. Yeast one-hybrid analysis confirms MAT1-1-1 binding to MAT1.1. Yeast strains were grown on SD-ura-leu in order to confirm the presence of both, a bait and a prey vector, after mating. *HIS3* reporter gene activity was analyzed on SD-ura-leu-his supplemented with 3-AT as indicated. *lacZ* reporter gene activity was analyzed using qualitative and quantitative β-galactosidase assays. A diploid strain harboring the mutated CPCR1 binding site BSIIm1 as a prey and the transcription factor CPCR1 as a bait construct was used as a negative control. A diploid strain carrying the native BSII binding site as a prey and CPCR1 as a bait is shown as a positive control (Schmitt *et al.*, 2004).

Previously successfully employed Y1H plasmids were used as a positive and negative control, and served as standard for quantitative β-galactosidase assays (Schmitt and Kück, 2000) (Fig. 7).

Y1H analysis confirmed binding of MAT1-1-1 to oligonucleotides Kex1-2, Ppg1-2, and Ppg1-2_m1 based on both, *HIS3* and *lacZ*, reporter gene activity. Moreover, quantitative β-galactosidase assays confirmed our results obtained from Shift–Western assays using oligonucleotide Ppg1-2_m1. In both analyses, binding between MAT1-1-1 and the oligonucleotide was reduced due to a single point mutation within one copy of MAT1.1. As integration of Ppg1-2_m2 into the prey vector pHISi led to transactivation with the empty bait vector pGADT7, Y1H analysis did not yield reliable results in this particular case. Most probably, this activation was mediated by a yeast protein that binds with high affinity to the mutated binding sequence. Additional control experiments were performed to exclude transactivation between pGADT7 and the remaining prey vectors (Fig. S7).

DsRed reporter gene assays confirm MAT1-1-1 binding to the kex1 and ppg1 promoter sequence in vivo

To further verify binding between MAT1-1-1 and the promoter regions of *kex1* and *ppg1 in vivo*, we performed *DsRed* reporter gene assays in *P. chrysogenum*. For this purpose, reporter gene constructs carrying the *DsRed* gene under control of the upstream sequence of *kex1* and *ppg1* were transformed into *P. chrysogenum* recipients MAT1-ChIP and P2niaD18, and plasmid integration was confirmed using PCR analysis. A plasmid containing the *DsRed* gene without a promoter sequence (pDsRed) was integrated into MAT1-ChIP as a control. As MAT1-ChIP contained the P_{gpd}::*egfp*::*MAT1-1-1* overexpression construct used for ChIP analysis, all derivatives of this strain showed clear nuclear EGFP signals, while no signals were detectable in the P2niaD18 background. *DsRed* expression in MAT1-ChIP+P_{ppg1}::*DsRed* and MAT1-ChIP+P_{kex1}::*DsRed* confirmed binding of the MAT1-1-1 protein to the promoter regions of *kex1* and *ppg1*, while no fluorescence was recorded for the MAT1-ChIP+pDsRed control strain (Fig. 8). Because only weak DsRed fluorescence was detectable for P_{kex1}::*DsRed* in P2niaD18 and no DsRed fluorescence was detectable for P2niaD18+P_{ppg1}::*DsRed*, overall activation of reporter gene expression could be clearly attributed to high *MAT1-1-1* gene expression in the MAT1-ChIP background. Thus, fluorescence microscopy confirmed the *in vivo* specificity of MAT1-1-1 binding to promoter regions of *kex1* and *ppg1*.

Characterization of a MAT1-1-1 target gene that functions beyond sexual development

To further validate functionality of a new MAT1-1-1 target gene, identified in our ChIP-seq approach and unlikely to be involved in regulation of sexual development, we generated *artA* (*Pc18g03940*) deletion strains (ΔartA) by homolog integration of a P_{trpC}-*nat1* resistance cassette

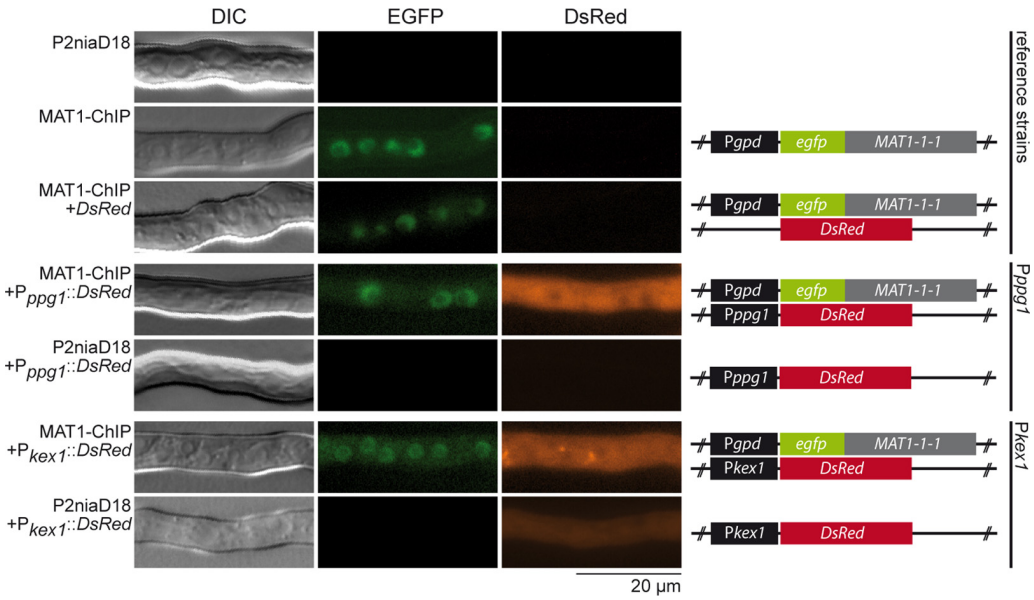

Fig. 8. *In vivo DsRed* reporter gene analysis confirms MAT1-1-1 binding to selected target gene promoter regions. Reporter gene constructs carrying the *DsRed* gene under control of the upstream sequence of *kex1* and *ppg1* (P_{kex1}: 1445 nt; P_{ppg1}: 843 nt) were transformed into *P. chrysogenum* strains MAT1-ChIP and P2niaD18. Fluorescence microscopy confirmed EGFP-MAT1-1-1 expression and nuclear localization in the MAT1-ChIP background. DsRed protein expression confirmed binding of MAT1-1-1 to the respective promoter regions. Scale bar = 20 µm.

in ΔKu70FRT2 background. Correct integration of the knockout construct was verified using PCR analysis. *ArtA* codes for a 14-3-3 family protein, which was previously shown to be involved in a pathway controlling conidiospore germination in *A. nidulans* (Kraus *et al.*, 2002). As shown in Fig. 9A, deletion of the corresponding homolog in *P. chrysogenum* results in a severe reduction in conidiospore germination (~ 30% germination after 24 h), when compared with the recipient ΔKu70FRT2 and wild type P2niaD18 (~ 90% germination after 24 h). This effect was further verified using microscopic analysis, confirming an impaired growth in ΔartA compared with the reference strains after 24 h of cultivation (Fig. 9B).

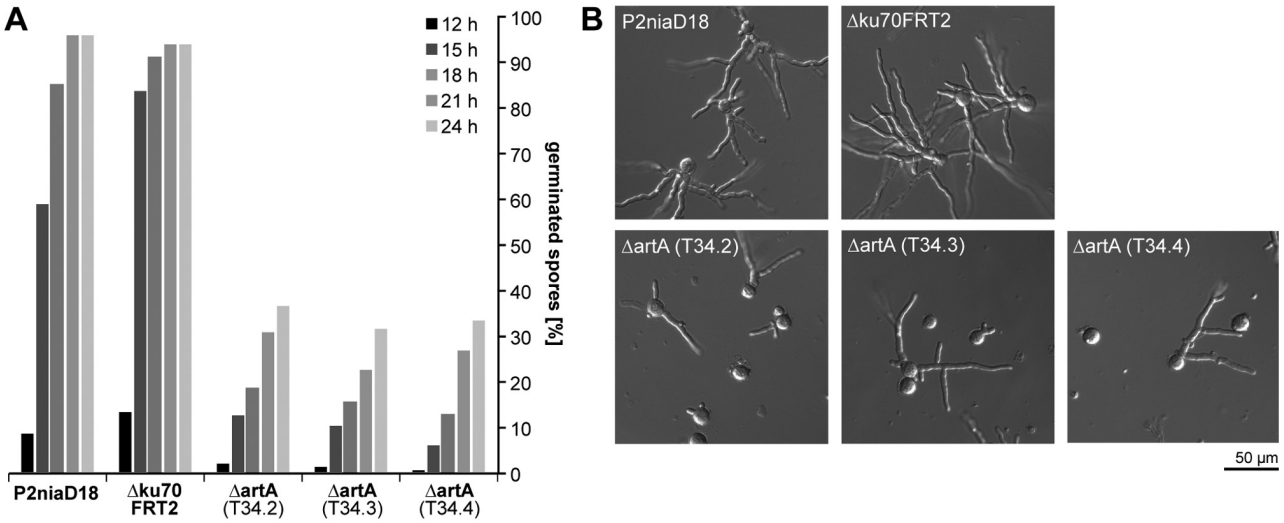

Fig. 9. Characterization of *artA* deletion strains.
A. Three independent *artA* deletion (ΔartA) mutants, recipient ΔKu70FRT2, and wild type P2niaD18 were grown on solid CCM. For each time point 400 conidiospores from each strain were investigated for determination of germination rates after 12, 15, 18, 21, and 24 h (given in %).
B. Microscopic analysis of strains used in (A) after 24 h of cultivation. Scale bar = 50 µm.

Discussion

ChIP-seq analysis identifies MAT1-1-1 target genes that have functions other than for sexual development

Although concerted research efforts have been made to analyze regulatory circuits controlled by mating-type-encoded TFs, little is still known about their specific target genes. Our work expands the current understanding of mating-type protein functions far beyond the regulation of sexual development alone, and provides unambiguous evidence for a participation of the mating-type α-domain TF MAT1-1-1 in regulation of asexual development and morphogenesis, as well as amino acid, iron and secondary metabolism in *P. chrysogenum*. Furthermore, we present the first genome-wide analysis focusing on unraveling the transcriptional regulatory network controlled by a mating-type locus-encoded TF and the comprehensive characterization of a MAT1-1-1 DNA-binding motif in euascomycetes.

Identification of *Pc14g01160* and *Pc22g15650* as MAT1-1-1 specific target genes confirms the biological significance of our ChIP-seq analyses, as they are homologs of *S. cerevisiae MFα1* and *STE3*, respectively, both αsgs (Galgoczy *et al*., 2004). Since their corresponding peak regions revealed significantly high statistical peak values, these observations are consistent with the general acceptance that the most highly bound regions in ChIP experiments occur near generally known functional targets, while many of the regions bound at much lower levels may represent 'non-functional' binding sites (Todeschini *et al*., 2014). Nevertheless, low-affinity TF binding may have a functional role in chromatin remodeling (Cao *et al*., 2010) or nucleosome positioning (Zaret and Carroll, 2011), which can influence gene expression at later developmental stages or have an additional non-transcriptional function (Spitz and Furlong, 2012).

We used previous microarray data (Böhm *et al*., 2013), which identified a total of 2421 genes as MAT1-1-1-dependent in a *MAT1-1-1* deletion strain (ΔMAT1) compared with wild type P2niaD18, to align ChIP-seq results and expression profiles of putative MAT1-1-1 target genes, identified in our ChIP-seq analysis. This comparison revealed an overlap of 29.9% (76/254), which is consistent to comparisons between TF binding events and expression profiling data in yeast and higher eukaryotes, showing a relatively small overlap of ~ 50% and 10–25% between TF occupancy and expression of neighboring genes (Spitz and Furlong, 2012). Nevertheless, our assumption that most of the 243 MAT1-1-1 binding sites identified in ChIP-seq experiments affect the expression of neighboring genes at some point during development was strengthened when *DsRed* reporter gene assays showed that MAT1-1-1 binding to promoter regions, identified as specific target regions in ChIP-seq analyses (P_{ppg1}, P_{kex1}), can be used for controlled expression of downstream reporter genes in a MAT1-1-1-dependent manner. Furthermore, DNA-binding assays and qRT-PCR analyses confirmed functionality of at least 13 non-mating-related MAT1-1-1 target genes, identified in our ChIP-seq approach and covering the functional categories morphogenesis and development, amino acid and secondary metabolism, iron metabolism as well as TFs. Important examples are the spore wall fungal hydrophobin encoding *dewA*, the non-ribosomal peptide synthetase encoding *sidD*, the bZIP TF encoding *atf21* and the F-box domain protein encoding *Pc22g22160*. Moreover, functional characterization of *artA*, a further MAT1-1-1 target gene, confirmed its role in regulation of conidiospore germination in *P. chrysogenum*. A comparable function was previously shown for *A. nidulans* (Kraus *et al*., 2002). This observation supports our hypothesis that MAT1-1-1 functions on a genome-wide level are more far-ranging than expected, and that the number of primary MAT1-1-1 target genes might be significantly higher than previously assumed. To improve clarity, all MAT1-1-1 target genes, verified by EMSAs and/or qRT-PCR analysis, are labeled with an asterisk (*) throughout this discussion (see Table 2 for further information).

Interestingly, none of the identified MAT1-1-1 target genes, assigned to sexual development in *P. chrysogenum*, showed MAT1-1-1-dependent changes in expression profiles in microarray analysis comparing ΔMAT1 to wild type P2niaD18, except for *kex1** and the homolog of *pac2* (*Pc12g15890*). *Pac2* encodes a cAMP-independent regulatory protein, modulating onset of sexual development in *S. pombe* and *M. oryzae*, and regulation of sporulation in *Ashbya gossypii* (Kunitomo *et al*., 1995; Wasserstrom *et al*., 2013; Chen *et al*., 2014). On the contrary, qRT-PCR analysis revealed a significant upregulation of *pre1**, *kex1**, and *ppg1** expression in a MAT1-1-1 overexpression strain (MAT1-ChIP) and significant downregulation of *pre1** in ΔMAT1 compared with P2niaD18 after 48 h of cultivation in shaking cultures. Accordingly, *pre1** and *ppg1** expression was shown to be significantly downregulated in ΔMAT1 compared with the parental strain after 72 h of cultivation in liquid shaking cultures (Böhm *et al*., 2013). These findings are consistent with reports, demonstrating that expression of pheromone precursor genes, and most probably receptor genes, is controlled by mating-type gene expression in heterothallic species, e.g. *N. crassa* (Kim and Borkovich, 2006). The overexpression of *MAT1-1-1* thus has an impact on the expression of genes involved in regulation and onset of sexual reproduction. Similar observations were made in *A. nidulans* and *N. crassa*, in which sexual reproduction correlates significantly with an increased expression of mating-type genes and key genes of a pheromone-response MAP-kinase signaling pathway (Paoletti *et al*.,

2007; Wang *et al*., 2014). However, deletion of *MAT1-1-1* in *P. chrysogenum* does not lead to significant changes in expression levels of key genes from the pheromone-response signaling pathway at early developmental stages, suggesting that these are, to a certain degree, independent of MAT1-1-1.

A significant number of MAT1-1-1 target genes, identified in our ChIP-seq analyses, might be involved in the manifestation of the phenotypic characteristics of *MAT1-1-1* overexpression and deletion strains, showing altered polarity of germinating hyphae, unusual branching behavior, and impaired hyphal growth and pellet formation (Böhm *et al*., 2013). Examples are *dewA** (*Pc16g06690*), encoding a spore wall fungal hydrophobin responsible for hydrophobicity of conidiospores in *A. nidulans* (Stringer and Timberlake, 1995; Grünbacher *et al*., 2014), *artA** (*Pc18g03940*), coding for a 14-3-3 family protein involved in regulation of polarization of germinating conidiospores in *A. nidulans* (Kraus *et al*., 2002), and *PAG1* (*Pc21g20900*), encoding a cell morphogenesis protein related to polarized morphogenesis and proliferation in *S. cerevisiae* (Du and Novick, 2002; Nelson *et al*., 2003). Furthermore, genes assigned to the formation of conidiospores were identified and showed significant upregulation in ΔMAT1, e.g. *atf21** (*Pc22g26820*) and *Pc19g00140**. *Atf21** codes for a basic leucine zipper (bZIP) TF and repressor of sexual development in *A. nidulans* (Lara-Rojas *et al*., 2011), while *Pc19g00140** shows high similarity to trehalose-6-phosphate synthase subunit encoding genes from *Aspergilli*, involved in the biosynthesis of trehalose, a compound necessary for long-term viability of fungal spores (Elbein *et al*., 2003). As formation of conidiospores is generally accepted to be restricted to asexual development, this observation fits the notion of MAT1-1-1 being a positive regulator of sexual reproduction and a negative regulator of asexual development. Consistent with this hypothesis is our recent finding that sporulation was increased by about 25% in a Δ*MAT1-1-1* strain compared with wild type (Böhm *et al*., 2013).

It is known that the developmental decision between sexual and asexual reproduction in *A. nidulans* is dependent on environmental factors, such as nutritional status and culture conditions (Han *et al*., 2003). Consequently, in most out-crossing ascomycetes, such as *N. crassa* and *S. cerevisiae*, nitrogen limitation is a key inducing condition for mating or sexual sporulation (Glass and Lorimer, 1991). As we identified *meaB** (*Pc18g00880*), a bZIP TF involved in regulation of expression of nitrogen-dependent genes in *A. nidulans* (Wong *et al*., 2007), as a target gene of MAT1-1-1 in ChIP-seq analyses and microarray analysis indicated upregulation in ΔMAT1 compared with wild type, MAT1-1-1 seems to act as a negative regulator of *meaB** expression in *P. chrysogenum*, thus, supporting the idea of nitrogen limitation as a key feature of induction of sexual reproduction in *P. chrysogenum*.

We found a variety of MAT1-1-1 target genes linked to amino acid and secondary metabolism, most of them showing downregulation in ΔMAT1 compared with wild type. *Pc18g02620*, encoding a cyanide hydratase/nitrilase, and *Pc22g18630**, encoding an enzyme catalyzing the chemical reaction of L-homocysteine to L-methionine, are important candidates, as they might have a direct impact on penicillin biosynthesis, which starts with the formation of a tripeptide based on L-cysteine, L-valine and L-α-aminoadipic acid. Several multidrug (*Pc12g00820*, *Pc16g06630*, *Pc16g11470*, *Pc20g03900*) and amino acid transporter encoding genes (*Pc06g01080*, *Pc22g06500*) complete this selection. As deletion of *MAT1-1-1* was shown to lead to a significant reduction in penicillin production (Böhm *et al*., 2013), these observations strengthen our idea of MAT1-1-1 being a positive regulator of secondary metabolism in *P. chrysogenum*.

Furthermore, integration of ChIP-seq and microarray data led to the identification of MAT1-1-1 target genes involved in iron transport and iron acquisition, e.g. *sidD** (*Pc22g20400*), encoding a non-ribosomal siderophore peptide synthetase important for biosynthesis of the intracellular siderophore triacetylfusarinine C (TAFC) (Schrettl *et al*., 2007), *fetC** (*Pc21g08020*), encoding for a ferroxidase, and *ftrA** (*Pc21g08030*), encoding for a high affinity iron permease that mediates uptake of Fe^{2+} during reductive iron acquisition (Schrettl and Haas, 2011). It is known from *Aspergillus* species that imbalance in iron homeostasis affects a variety of cellular functions, e.g. growth rates, germination, sensitivity of conidia to oxidative stress and formation of cleistothecia (Eisendle *et al*., 2006a). Furthermore, deletion of *sidD** in *A. fumigatus* was shown to lead to decreased conidiation during iron-depleted conditions (Schrettl *et al*., 2007), whereas deletion of *ftrA** displayed an eightfold increase in TAFC siderophore production under iron-depleted conditions, demonstrating that lack of FtrA brings forward the onset of siderophore production (Schrettl *et al*., 2004).

Identification of a new MAT1-1-1 DNA-binding motif

Using EMSAs, Shift–Western and Y1H analysis, we showed that MAT1-1-1 binds with high specificity to the newly identified MAT1.1 DNA-binding consensus sequence 'CTATTGAG'. The motif was further shown to be conserved among euascomycetes and showed similarities to known DNA-binding motifs of proteins known to be involved in regulation of sexual reproduction in yeast, e.g. MATa1, Mcm1, and Hcm1, and embryonic development in vertebrates, e.g. Sox9, Nkx2-5, and Sox17. Even though DNA-sequence recognition by TFs can be con-

served across large evolutionary distances, binding specificity of MATα1 has been shown to have changed substantially over small evolutionary distances (Tuch *et al.*, 2008). As our analysis pointed to obvious differences between MAT1-1-1 binding sites in euascomycetes and hemiascomycetes, especially *C. albicans*, these findings are consistent with the hypothesis that hemiascomycetes and euascomycetes share a common ancestor, but that binding specificity of modern MATα1 proteins from *C. albicans* and euascomycetes might have changed substantially during evolution (Baker *et al.*, 2011).

The strongest protein–DNA interaction was observed between MAT1-1-1 and an oligonucleotide probe harboring two copies of the MAT1.1 binding motif, forming the imperfect palindrome 5′-TCAATA-N_7-TATTGA-3′. Correspondingly, the strongest interaction between DNA and MAT1-1-1, as deduced from ChIP-seq data, was observed for those peak regions characterized by a noticeable high frequency of MAT1.1 with close matches to the consensus sequence, whereas weak interactions were characterized by a relatively low abundance of the motif (compare with Table 2 and Dataset S1). Since eukaryotic TFs tend to recognize shorter DNA sequence motifs compared with bacterial TFs, clustering of sites is often required to achieve specific recognition (Wunderlich and Mirny, 2009).

Although a large number of MAT1-1-1 peak regions contained at least one copy of MAT1.1, some peaks completely lacked it. However, this might be due to statistical thresholds applied during motif prediction and motif detection procedures. On the other hand, this is a common observation: even if ChIP-seq peaks are typically enriched in the consensus motif for the TF in question, a significant proportion of peaks lacks clearly identifiable motifs (Robertson *et al.*, 2007; Valouev *et al.*, 2008). For example, the consensus sequence for E2F family proteins that control various cellular and organismal functions in higher eukaryotes is present in less than 20% of the regions recognized in ChIP-chip experiments in human and mouse cells (Rabinovich *et al.*, 2008). This observation might be ascribed to the fact that most TFs not only interact with DNA through a consensus site but also recognize divergent sequences. For example, a study of approximately 100 mouse TF revealed that almost half of these proteins can recognize several different sequences in addition to the known DNA-binding consensus sequences (Badis *et al.*, 2009). Furthermore, specific recognition of regulatory elements by a TF is strongly influenced by its ability to interact with other proteins that bind to neighboring DNA sites. The simplest example of this mechanism is the formation of TF dimers or higher order structures (Amoutzias *et al.*, 2008). Since cooperative binding was described for the mating-type α1 HMG domain TF and Mcm1 from *S. cerevisiae* (Carr *et al.*, 2004; Baker *et al.*, 2011), dimerization might also be a regulatory feature of MAT1-1-1 in *P. chrysogenum*.

Interestingly, the most prominent MAT1-1-1 target genes, characterized by high statistical peak values combined with an accumulation of MAT1.1 ($p \leq 0.001$), were assigned to sexual reproduction. This finding might indicate a regulatory feature ensuring high-affinity binding of MAT1-1-1 to the corresponding promoter regions, even under conditions where only a low amount of MAT1-1-1 protein is available. Moreover, the occurrence of MAT1.1 within the upstream regions of new direct MAT1-1-1 target genes presented within this work points to an evolutionary link between mating and other cellular functions which were believed to be independent of MAT1-1-1 protein functions until now. This hypothesis was further strengthened by EMSAs and qRT-PCR analyses, verifying functionality of selected MAT1-1-1 target genes identified in our ChIP-seq approach. Further research is needed to identify interaction partners of MAT1-1-1 on protein level and to understand interactions between the TF, enhancer elements and other *cis*-regulatory elements. Furthermore, as our analysis was designed to identify as many MAT1-1-1 target genes as possible, further studies, however, will be needed in order to decipher MAT1-1-1 mediated transcriptional regulation under control of its native promoter sequence, e.g. as a function of developmental stages or physiological culture conditions.

Taken together, our discoveries concerning the sexual biology of *P. chrysogenum* presented within this work greatly advance the current understanding of sexual reproduction within ascomycetes, and open up new avenues for the study of fungal development as a whole. Based on our finding that the mating-type encoded TF MAT1-1-1 not only regulates expression of αsgs related to sexual reproduction but also other key biological processes, it appears that mating-type regulated transcriptional networks have undergone drastic reorganization, resulting in the presence of DNA binding sites in the promoters of – at first glance – unrelated target genes that are bound and controlled by highly conserved transcriptional regulators in different fungi. This hypothesis is supported by a recent discovery showing that targets of the mating-type TF heterodimer Sxi2a-Sxiα1 from *Cryptococcus neoformans* not only include genes known to be involved in sexual reproduction but also several well studied virulence genes (Mead *et al.*, 2015). Microarray analyses in other euascomycetes also pointed to an unexpectedly large number of genes that are expressed in a mating-type dependent manner (Lee *et al.*, 2006; Pöggeler *et al.*, 2006; Keszthelyi *et al.*, 2007; Bidard *et al.*, 2011). In combination, these data suggest that mating-type protein regulatory functions might reach far beyond sexual development in these species as well. Future research will be necessary in order to determine

exactly which changes in MAT1-1-1 and its corresponding DNA binding site were necessary to allow for the expansion in MAT1-1-1 regulatory functions during evolution.

The observation that MAT1-1-1 is involved in regulation of development, morphogenesis and metabolism in *P. chrysogenum* supports the idea that *MAT* genes are functionally retained even during the asexual part of the life cycle and the apparent absence of a sexual phase, presumably because of the impact of positive selection on important processes unrelated to sexual development in asexual fungal populations (Ádám *et al*., 2011). Since we demonstrated that MAT1-1-1 regulates expression of a number of genes related to various traits of morphology and development, it is conceivable that the mating-type protein mediated regulation is necessary for efficient balance between morphologic features characteristic to the sexual and asexual parts of the life cycle. This might also be true for an involvement of MAT1-1-1 in regulation of secondary, amino acid and iron metabolism. It is known from various euascomycetes that there is a concerted balance between sexual development and secondary metabolism (Bayram *et al*., 2008; Hoff *et al*., 2010; Wiemann *et al*., 2010; Kopke *et al*., 2012). Another important example is fungal iron metabolism, which was shown to affect both asexual and sexual development (Eisendle *et al*., 2003; 2006b; Schrettl *et al*., 2007; Johnson, 2008). Since these traits are also crucial in terms of applied microbiology, our work will further not only contribute to the advanced improvement of *P. chrysogenum* strains used for industrial production of β-lactam antibiotics but also to other filamentous fungi with biotechnological relevance.

Experimental procedures

Strains and culture conditions

Penicillium chrysogenum strains (Table S1) were grown in shaking or surface cultures in complete culture medium (CCM; 0.3% (w/v) sucrose, 0.05% (w/v) NaCl, 0.05% (w/v) K_2HPO_4, 0.05% (w/v) $MgSO_4$, 0.001% (w/v) $FeSO_4$, 0.5% (w/v) tryptic soy broth, 0.1% (w/v) yeast extract, 0.1% (w/v) meat extract, 0.15% (w/v) dextrin, pH 7.0) at 27°C. For inoculation, 0.5×10^7 spores derived from cultures grown on M322 solid medium (0.35% (w/v) $(NH_4)_2SO_4$, 0.2% (w/v) KSO_4, 0.02% (w/v) $KHSO_4$, 1 g N/l soy flour, 0.5% (w/v) lime stone powder, 5% (w/v) lactose, pH 6.3) for 4–5 days were used. *Escherichia coli* strain XL1 blue was used for cloning and plasmid propagation purposes, while BL21 (DE3) served as a host for heterologous overexpression of MAT1-1-1 (Bullock *et al*., 1987; Miroux and Walker, 1996). *Saccharomyces cerevisiae* strains PJ69-4a and PJ69-4α were used for yeast one-hybrid analysis (James *et al*., 1996). Strains were grown at 30°C on synthetic defined (SD) medium lacking selected amino acids used for auxotrophy marker selection. Mating of PJ69-4a and -4α strains was performed in liquid yeast peptone dextrose adenine (YPDA) medium at 30°C and 50 rpm.

Construction of recombinant P. chrysogenum *strains*

For generation of strains used for ChIP-seq analysis, *DsRed* reporter gene assays and deletion mutants (Table S1), the corresponding plasmids (Table S2) were transformed into *P. chrysogenum* strain P2niaD18 and Δku70FRT2, respectively. Transformation was performed as described previously (Hoff *et al*., 2010; Kamerewerd *et al*., 2011) with some modifications. Cultures were grown for 72 h and protoplasts were transformed with circular plasmid DNA for ectopic, and linear plasmid DNA for homologous integration. Transformants were selected on CCM media containing 150 μg mL^{-1} nourseothricin (Werner BioAgents, Jena, Germany) and 40 μg ml^{-1} phleomycin (Invivogen, CA, USA) as necessary. Resistant colonies were isolated and tested for correct integration of plasmid DNA as previously described (Hoff *et al*., 2010).

Sample preparation for ChIP-seq

Chromatin immunoprecipitation (ChIP) was carried out essentially as described previously (Tamaru *et al*., 2003; Smith *et al*., 2011) with the following modifications. *P. chrysogenum* strains were grown in 100 mL CCM cultures inoculated with 0.5×10^7 spores for 48 h at 120 rpm and 27°C. For chromatin fixation, freshly prepared formaldehyde (in NaOH) was added to a final concentration of 1%, and cultures were incubated at 27°C and 100 rpm for 30 min. Five milliliters of 2.5 M glycine was added to quench formaldehyde, and cultures were incubated at room temperature with gentle shaking for 5 min. Approximately 250 mg mycelium were resuspended in 750 μL lysis buffer (50 mM HEPES–KOH pH 7.5, 90 mM NaCl, 1 mM ethylenediaminetetraacetic acid (EDTA), 1% Triton X-100, 0.1% sodium deoxycholate (DOC) supplemented with fresh protease inhibitors) and chromatin was sheared using a Branson 250 sonifier (output 2, duty cycle 0.8, 6 × 20 impulses). After pre-clearing with protein A agarose beads (Invitrogen, Darmstadt, Germany) the soluble chromatin fraction was immunoprecipitated using anti-GFP antibody (ab290; Abcam, Cambridge, UK). Fresh protein A agarose beads were added to bind antibody–protein–DNA complexes. The supernatant was discarded and beads were washed several times (1 × TE buffer: 10 mM Tris–HCl pH 8.8, 1 mM EDTA; 2 × lysis buffer without protease inhibitors; 1 × lysis buffer without protease inhibitors + 0.5 M NaCl; 1 × LiCl wash buffer: 0.25 M LiCl, 1 mM EDTA, 10 mM Tris–HCl pH 8.0, 0.5% NP-40, 0.5% DOC). Beads were incubated two times in TE(S) (50 mM Tris–HCl pH 8.0, 10 mM EDTA, 1% SDS) at 65°C for 10 min with gentle agitation to elute protein–DNA complexes. To reverse the crosslinking, samples were incubated at 65°C for 6–16 h. After RNaseA and ProteinaseK digestion, DNA from immunoprecipitated chromatin (ChIP-DNA) and input samples (input-DNA) was isolated. Construction of ChIP-libraries and sequencing of 50 nt single-end reads on a Illumina HiSeq 2000 were performed by GATC Biotech AG (Konstanz, Germany) or at the OSU CGRB core facility.

Data analysis and visualization

Sequences corresponding to adaptors were removed from reads, and remaining sequences were subsequently mapped

to the latest version of the *P. chrysogenum* P2niaD18 genome (Specht *et al*., 2014) using Bowtie version 1.0.1 (Langmead *et al*., 2009) with the following settings: '–S –q –m 1', which only retains unique alignments. Binary Alignment/Map (BAM) files were sorted and indexed using SAMtools (Li *et al*., 2009), and visualized using the Integrative Genomics Viewer (IGV) (Thorvaldsdóttir *et al*., 2012). A genome-wide distribution figure of MAT1-1-1 binding sites is provided in Fig. S8. Further data analysis was performed using the HOMER software for motif discovery and next-generation sequencing analysis (Heinz *et al*., 2010). Quality control analysis included examination of clonal tag counts in order to determine the non-redundant fraction of mapped reads, autocorrelation analysis to enable sequencing fragment length estimation, nucleotide frequency analysis and fragment GC % distribution to rule out sequence biases and analysis of ChIP-fragment density near MAT1-1-1-specific peak regions. Peaks were called using findPeaks.pl using the -style factor option, a FDR ≤ 0.001, and a *p*-value over local background cutoff of 1.00e–04. Peak regions for each individual experiment were intersected using mergePeaks.pl –d 100, reporting peaks within a maximum distance of 100 nt as overlapping. Peaks were assigned to neighboring and overlapping genes using a custom-made Perl script based on BioPerl modules and blast2go analysis (Conesa *et al*., 2005). Functional category enrichment analysis of genes associated with peaks was performed using the MIPS functional catalogue database (FunCat) (Ruepp *et al*., 2004). Raw sequencing data from ChIP experiments are available from the NCBI SRA database (http://www.ncbi.nlm.nih.gov/sra), study ID PRJNA257456, Accession # SRP045261.

Sequence motif analysis

The central 100 nt region of selected MAT1-1-1 peak regions was submitted to MEME (Multiple Em for Motif Elicitation; http://meme.nbcr.net/meme/) (Bailey and Elkan, 1994) for *de novo* motif prediction. Further analysis was performed using CentriMo (Bailey and Machanick, 2012) and FIMO (Grant *et al*., 2011). For comparison of the newly identified MAT1-1-1 DNA-binding consensus sequence against the JASPAR CORE (2014) fungi and vertebrates databases, results were submitted to TOMTOM (Gupta *et al*., 2007) using default parameters.

Expression and purification of recombinant GST-MAT1-1-1 protein

The *MAT1-1-1* cDNA sequence was integrated into the expression vector pGEX-4T3 (Amersham Bioscience, Freiburg, Germany) to generate plasmid pGEX-MAT1 (see Table S2). GST and GST-MAT1-1-1 were purified from *E. coli* BL21 (DE3) cells. Purification of recombinant protein and GST alone was performed as described earlier using an elution buffer containing 50 mM Tris/HCl, 30 mM reduced glutathione, 100 mM NaCl, pH 8.0 (Janus *et al*., 2007). Purified protein was supplemented with 87% glycerol and stored at −70°C until used for further applications.

Quantification of protein levels and immunodetection

The concentration of purified GST-MAT1-1-1 and GST alone was determined by using Bradford reagent (BioRad, München, Germany). Western blotting and immunodetection of GST-tagged proteins were performed using RPN1236 anti-GST HRP conjugate (GE Healthcare, Freiburg, Germany). Detection of GFP-MAT1-1-1 from *P. chrysogenum* total protein isolates was performed using JL-8 antibody to GFP (Clontech, Saint-Germain-en-Laye, France) and HRP-coupled secondary antibody #7076 (Cell Signaling Technology, Leiden, The Netherlands).

Electrophoretic mobility shift assays (EMSAs) and Shift–Western analysis

Gel shift assays were performed using oligonucleotides derived from ChIP-enriched regions and purified GST-MAT1-1-1. Double-stranded oligonucleotides were 5′-end-labeled using polynucleotide kinase (Roche, Basel, Switzerland) and [γ-32P]-ATP (Hartmann Analytic, Braunschweig, Germany). For shift experiments, 3.5–7.0 fmol (~ 50–100 cps) of radiolabeled oligonucleotides was incubated with varying protein concentrations in the presence of 2 μL binding buffer (250 mM Tris/HCl pH 8.0, 1 M KCl, 50 % glycerol) and 1 μg poly(dI-dC)-poly(dI-dC) (Affymetrix USB, CA, USA) in a total volume of 20 μL for 20 min at room temperature. Samples were run on 5% polyacrylamide gels at 4°C in 190 mM glycine, 27 mM Tris/HCl pH 8.5. Competition experiments were performed by adding unlabeled oligonucleotide. Preparation of gels used for Shift–Western analysis (Demczuk *et al*., 1993) was performed as described earlier. Denaturation of proteins and blotting to a PVDF membrane (PerkinElmer, MA, USA) was performed as described previously (Granger-Schnarr *et al*., 1988) with a transfer time of 180 min at 1.3 A and a transfer buffer containing 25 mM Tris, 192 mM glycine and 10 % methanol. The sequences of all oligonucleotides used for shift analyses are provided in Table S3.

Nucleic acids isolation, cDNA synthesis, quantitative RT-PCR and ChIP-PCR

Isolation of nucleic acids, cDNA synthesis and qRT-PCR analysis were carried out as described earlier (Hoff *et al*., 2009; Böhm *et al*., 2013). ChIP-PCR analysis was performed as described for qRT-PCR analysis, using ChIP- and input-DNA from independent ChIP experiments as a template. The sequences of all oligonucleotides used for PCR analyses are given in Table S3.

Microarray data analysis

Analysis of microarray data was performed as described previously using the affylmGUI R package (Wettenhall *et al*., 2006; Wolfers *et al*., 2014). *p*-Values for single time points were generated by treating datasets from light-grown ΔMAT1 (48 h, 60 h, 96 h) as independent biological replicates.

Yeast one-hybrid analysis

Complementary oligonucleotides harboring three copies of the corresponding oligonucleotide sequence used for EMSAs were cloned into plasmids pHISi and pLacZi to generate prey vectors for yeast one-hybrid analysis (see Table S3), as described previously (Schmitt and Kück, 2000). As a bait, the MAT1-1-1 cDNA sequence was integrated into plasmid pGADT7 to generate plasmid pMAT1-AD (see Table S2). Bait and prey vectors were transferred into *S. cerevisiae* strains PJ69-4α and PJ69-4a, respectively. Diploid reporter strains harboring both, the bait and a prey vector, were generated by mating. For analyzing DNA–protein interactions between MAT1-1-1 and putative DNA-binding sites, reporter strains were tested for growth on -his/-leu/-ura selective media supplemented with 3-amino-1,2,4-triazole (3-AT) (Merck, Darmstadt, Germany) as indicated. Further, β-galactosidase activity of reporter strains was analyzed by qualitative and quantitative determination of 5-bromo-4-chloro-3-indolyl-beta-D-galactopyranoside and *O*-nitrophenyl β-d-galactopyranoside turnover, respectively.

Microscopy

P. chrysogenum strains were grown on glass slides with a thin layer of CCM at 27°C. Fluorescence and light microscopy was carried out with an AxioImager M1 fluorescence microscope (Zeiss, Jena, Germany) using a SPECTRA Light Engine® LED lamp (Lumencor, OR, USA) as described previously (Engh *et al*., 2007). Images were captured with a Photometrix Cool SnapHQ camera (Roper Scientific, AZ, USA) and MetaMorph software version 6.3.1. Recorded images were edited with MetaMorph and Adobe Photoshop CS4. Counter staining of nuclei was performed using NucBlue® Live Cell Stain (Life Technologies GmbH, Darmstadt, Germany) as specified by the manufacturer. Pellet quantification assays were conducted as described earlier (Böhm *et al*., 2013).

Multiple sequence alignments

Multiple sequence alignments were performed using the Guidance server (http://guidance.tau.ac.il/) and MAFFT default settings (Penn *et al*., 2010). Alignments were visualized using Jalview according to the Clustalx color scheme (http://www.jalview.org/) (Waterhouse *et al*., 2009).

Acknowledgements

We thank L. Connolly, Dr. J. Galazka, Dr. E. Bredeweg, S. Friedman and M. Dasenko for help with ChIP-seq analyses, PD Dr. M. Nowrousian, M. Sc. T. A. Dahlmann and M. Sc. D. Terfehr for help with bioinformatics, and I. Godehardt for technical assistance. We thank Dr. I. Zadra, Dr. H. Kürnsteiner, Dr. E. Friedlin, and Dr. T. Specht for their ongoing interest and support, and Dr. I. Teichert for critical reading of the manuscript. This work was funded by Sandoz GmbH, the Christian Doppler Society, the German National Academic Foundation, and the Ruhr-University Bochum Research School.

The authors declare no conflict of interest.

Author contributions

K.B., U.K., M.F. designed experiments; K.B., C.B. performed experiments; K.B. analyzed data; K.B., U.K., M.F. wrote the manuscript. All authors discussed results and commented on the manuscript.

References

Ádám, A.L., García-Martínez, J., Szücs, E.P., Avalos, J., and Hornok, L. (2011) The MAT1-2-1 mating-type gene upregulates photo-inducible carotenoid biosynthesis in *Fusarium verticillioides*. *FEMS Microbiol Lett* **318:** 76–83.

Amoutzias, G.D., Robertson, D.L., Van de Peer, Y., and Oliver, S.G. (2008) Choose your partners: dimerization in eukaryotic transcription factors. *Trends Biochem Sci* **33:** 220–229.

Badis, G., Berger, M.F., Philippakis, A.A., Talukder, S., Gehrke, A.R., Jaeger, S.A., *et al*. (2009) Diversity and complexity in DNA recognition by transcription factors. *Science* **324:** 1720–1723.

Bailey, T.L., and Elkan, C. (1994) Fitting a mixture model by expectation maximization to discover motifs in biopolymers. *Proc Int Conf Intell Syst Mol Biol* **2:** 28–36.

Bailey, T.L., and Machanick, P. (2012) Inferring direct DNA binding from ChIP-seq. *Nucleic Acids Res* **40:** e128.

Baker, C.R., Tuch, B.B., and Johnson, A.D. (2011) Extensive DNA-binding specificity divergence of a conserved transcription regulator. *Proc Natl Acad Sci USA* **108:** 7493–7498.

Baker, C.R., Booth, L.N., Sorrells, T.R., and Johnson, A.D. (2012) Protein modularity, cooperative binding, and hybrid regulatory states underlie transcriptional network diversification. *Cell* **151:** 80–95.

Bayram, Ö., Krappmann, S., Ni, M., Bok, J.W., Helmstaedt, K., Valerius, O., *et al*. (2008) VelB/VeA/LaeA complex coordinates light signal with fungal development and secondary metabolism. *Science* **320:** 1504–1506.

Bender, A., and Sprague, G.F., Jr (1987) MAT alpha 1 protein, a yeast transcription activator, binds synergistically with a second protein to a set of cell-type-specific genes. *Cell* **50:** 681–691.

Bidard, F., Ait Benkhali, J., Coppin, E., Imbeaud, S., Grognet, P., Delacroix, H., and Debuchy, R. (2011) Genome-wide gene expression profiling of fertilization competent mycelium in opposite mating types in the heterothallic fungus *Podospora anserina*. *PLoS ONE* **6:** e21476.

Böhm, J., Hoff, B., O'Gorman, C.M., Wolfers, S., Klix, V., Binger, D., *et al*. (2013) Sexual reproduction and mating-type-mediated strain development in the penicillin-producing fungus *Penicillium chrysogenum*. *Proc Natl Acad Sci USA* **110:** 1476–1481.

Bullock, W.O., Fernandez, J.M., and Short, J.M. (1987) XI1-Blue – a high-efficiency plasmid transforming reca *Escherichia coli* strain with beta-galactosidase selection. *Biotechniques* **5:** 376–378.

Cao, Y., Yao, Z., Sarkar, D., Lawrence, M., Sanchez, G.J., Parker, M.H., *et al*. (2010) Genome-wide MyoD binding in skeletal muscle cells: a potential for broad cellular reprogramming. *Dev Cell* **18:** 662–674.

Carr, E.A., Mead, J., and Vershon, A.K. (2004) Alpha1-induced DNA bending is required for transcriptional activation by the Mcm1-alpha1 complex. *Nucleic Acids Res* **32:** 2298–2305.

Chen, C.Y., and Schwartz, R.J. (1995) Identification of novel DNA binding targets and regulatory domains of a murine tinman homeodomain factor, Nkx-2.5. *J Biol Chem* **270:** 15628–15633.

Chen, Y., Zhai, S., Zhang, H., Zuo, R., Wang, J., Guo, M., *et al*. (2014) Shared and distinct functions of two Gti1/Pac2 family proteins in growth, morphogenesis and pathogenicity of *Magnaporthe oryzae*. *Environ Microbiol* **16:** 788–801.

Conesa, A., Götz, S., García-Gómez, J.M., Terol, J., Talón, M., and Robles, M. (2005) Blast2GO: a universal tool for annotation, visualization and analysis in functional genomics research. *Bioinformatics* **21:** 3674–3676.

Coppin, E., and Debuchy, R. (2000) Co-expression of the mating-type genes involved in internuclear recognition is lethal in *Podospora anserina*. *Genetics* **155:** 657–669.

Debuchy, R., Berteaux-Lecellier, V., and Silar, P. (2010) Mating systems and sexual morphogenesis in ascomycetes. In *Cellular and Molecular Biology of Filamentous Fungi*. Washington, DC: ASM Press, pp. 501–535.

Demczuk, S., Harbers, M., and Vennstrom, B. (1993) Identification and analysis of all components of a gel retardation assay by combination with immunoblotting. *Proc Natl Acad Sci USA* **90:** 2574–2578.

DeZwaan, T.M., Carroll, A.M., Valent, B., and Sweigard, J.A. (1999) *Magnaporthe grisea* Pth11p is a novel plasma membrane protein that mediates appressorium differentiation in response to inductive substrate cues. *Plant Cell* **11:** 2013–2030.

Dmochowska, A., Dignard, D., Henning, D., Thomas, D.Y., and Bussey, H. (1987) Yeast KEX1 gene encodes a putative protease with a carboxypeptidase B-like function involved in killer toxin and alpha-factor precursor processing. *Cell* **50:** 573–584.

Du, L.L., and Novick, P. (2002) Pag1p, a novel protein associated with protein kinase Cbk1p, is required for cell morphogenesis and proliferation in *Saccharomyces cerevisiae*. *Mol Biol Cell* **13:** 503–514.

Dyer, P.S., and O'Gorman, C.M. (2012) Sexual development and cryptic sexuality in fungi: insights from *Aspergillus* species. *FEMS Microbiol Rev* **36:** 165–192.

Eisendle, M., Oberegger, H., Zadra, I., and Haas, H. (2003) The siderophore system is essential for viability of *Aspergillus nidulans*: functional analysis of two genes encoding l-ornithine N 5-monooxygenase (*sidA*) and a nonribosomal peptide synthetase (*sidC*). *Mol Microbiol* **49:** 359–375.

Eisendle, M., Schrettl, M., Kragl, C., Müller, D., Illmer, P., and Haas, H. (2006a) The intracellular siderophore ferricrocin is involved in iron storage, oxidative-stress resistance, germination, and sexual development in *Aspergillus nidulans*. *Eukaryot Cell* **5:** 1596–1603.

Eisendle, M., Schrettl, M., Kragl, C., Müller, D., Illmer, P., and Haas, H. (2006b) The intracellular siderophore ferricrocin is involved in iron storage, oxidative-stress resistance, germination, and sexual development in *Aspergillus nidulans*. *Eukaryot Cell* **5:** 1596–1603.

Elbein, A.D., Pan, Y.T., Pastuszak, I., and Carroll, D. (2003) New insights on trehalose: a multifunctional molecule. *Glycobiology* **13:** 17R–27R.

Engh, I., Würtz, C., Witzel-Schlomp, K., Zhang, H.Y., Hoff, B., Nowrousian, M., *et al*. (2007) The WW domain protein PRO40 is required for fungal fertility and associates with woronin bodies. *Eukaryot Cell* **6:** 831–843.

Fukuda, K., Yamada, K., Deoka, K., Yamashita, S., Ohta, A., and Horiuchi, H. (2009) Class III chitin synthase ChsB of *Aspergillus nidulans* localizes at the sites of polarized cell wall synthesis and is required for conidial development. *Eukaryot Cell* **8:** 945–956.

Galgoczy, D.J., Cassidy-Stone, A., Llinas, M., O'Rourke, S.M., Herskowitz, I., DeRisi, J.L., and Johnson, A.D. (2004) Genomic dissection of the cell-type-specification circuit in *Saccharomyces cerevisiae*. *Proc Natl Acad Sci USA* **101:** 18069–18074.

Glass, N.L., and Lorimer, I. (1991) More gene manipulations in fungi. In *Ascomycete Mating Types*. Bennett, J.W., and Lasure, L.S. (eds). San Diego: CA: Academic Press, pp. 193–216.

Granger-Schnarr, M., Lloubes, R., de Murcia, G., and Schnarr, M. (1988) Specific protein-DNA complexes: immunodetection of the protein component after gel electrophoresis and Western-blotting. *Anal Biochem* **174:** 235–238.

Grant, C.E., Bailey, T.L., and Noble, W.S. (2011) FIMO: scanning for occurrences of a given motif. *Bioinformatics* **27:** 1017–1018.

Grünbacher, A., Throm, T., Seidel, C., Gutt, B., Rohrig, J., Strunk, T., *et al*. (2014) Six hydrophobins are involved in hydrophobin rodlet formation in *Aspergillus nidulans* and contribute to hydrophobicity of the spore surface. *PLoS ONE* **9:** e94546.

Grzenda, A., Lomberk, G., Zhang, J.S., and Urrutia, R. (2009) Sin3: master scaffold and transcriptional corepressor. *Biochim Biophys Acta* **1789:** 443–450.

Gupta, S., Stamatoyannopoulos, J.A., Bailey, T.L., and Noble, W.S. (2007) Quantifying similarity between motifs. *Genome Biol* **8:** R24.

Haber, J.E. (2012) Mating-type genes and MAT switching in *Saccharomyces cerevisiae*. *Genetics* **191:** 33–64.

Han, K.H., Lee, D.B., Kim, J.H., Kim, M.S., Han, K.Y., Kim, W.S., *et al*. (2003) Environmental factors affecting development of *Aspergillus nidulans*. *J Microbiol* **41:** 34–40.

Heinz, S., Benner, C., Spann, N., Bertolino, E., Lin, Y.C., Laslo, P., *et al*. (2010) Simple combinations of lineage-determining transcription factors prime *cis*-regulatory elements required for macrophage and B cell identities. *Mol Cell* **38:** 576–589.

Herskowitz, I. (1989) A regulatory hierarchy for cell specialization in yeast. *Nature* **342:** 749–757.

Hoff, B., Kamerewerd, J., Sigl, C., Zadra, I., and Kück, U. (2009) Homologous recombination in the antibiotic producer *Penicillium chrysogenum*: strain ΔPcku70 shows up-regulation of genes from the HOG pathway. *Appl Microbiol Biotechnol* **85:** 1081–1094.

Hoff, B., Kamerewerd, J., Sigl, C., Mitterbauer, R., Zadra, I., Kürnsteiner, H., and Kück, U. (2010) Two components of a velvet-like complex control hyphal morphogenesis,

conidiophore development, and penicillin biosynthesis in *Penicillium chrysogenum*. *Eukaryot Cell* **9:** 1236–1250.
Irie, K., Nomoto, S., Miyajima, I., and Matsumoto, K. (1991) SGV1 encodes a CDC28/cdc2-related kinase required for a G alpha subunit-mediated adaptive response to pheromone in *S. cerevisiae*. *Cell* **65:** 785–795.
James, P., Halladay, J., and Craig, E.A. (1996) Genomic libraries and a host strain designed for highly efficient two-hybrid selection in yeast. *Genetics* **144:** 1425–1436.
Janus, D., Hortschansky, P., and Kück, U. (2007) Identification of a minimal *cre1* promoter sequence promoting glucose-dependent gene expression in the β-lactam producer *Acremonium chrysogenum*. *Curr Genet* **53:** 35–48.
Johnson, L. (2008) Iron and siderophores in fungal-host interactions. *Mycol Res* **112:** 170–183.
Julius, D., Brake, A., Blair, L., Kunisawa, R., and Thorner, J. (1984) Isolation of the putative structural gene for the lysine-arginine-cleaving endopeptidase required for processing of yeast prepro-*alpha*-factor. *Cell* **37:** 1075–1089.
Kamerewerd, J., Zadra, I., Kürnsteiner, H., and Kück, U. (2011) *PcchiB1*, encoding a class V chitinase, is affected by PcVelA and PcLaeA, and is responsible for cell wall integrity in *Penicillium chrysogenum*. *Microbiology* **157:** 3036–3048.
Kanai, Y., Kanai-Azuma, M., Noce, T., Saido, T.C., Shiroishi, T., Hayashi, Y., and Yazaki, K. (1996) Identification of two Sox17 messenger RNA isoforms, with and without the high mobility group box region, and their differential expression in mouse spermatogenesis. *J Cell Biol* **133:** 667–681.
Keszthelyi, A., Jeney, A., Kerényi, Z., Mendes, O., Waalwijk, C., and Hornok, L. (2007) Tagging target genes of the MAT1-2-1 transcription factor in *Fusarium verticillioides* (*Gibberella fujikuroi* MP-A). *Antonie Van Leeuwenhoek* **91:** 373–391.
Kim, H., and Borkovich, K.A. (2006) Pheromones are essential for male fertility and sufficient to direct chemotropic polarized growth of trichogynes during mating in *Neurospora crassa*. *Eukaryot Cell* **5:** 544–554.
Kopke, K., Hoff, B., Bloemendal, S., Katschorowski, A., Kamerewerd, J., and Kück, U. (2012) Members of the *Penicillium chrysogenum* velvet complex play functionally opposing roles in the regulation of penicillin biosynthesis and conidiation. *Eukaryot Cell* **12:** 299–310.
Kraus, P.R., Hofmann, A.F., and Harris, S.D. (2002) Characterization of the *Aspergillus nidulans* 14-3-3 homologue, ArtA. *FEMS Microbiol Lett* **210:** 61–66.
Krüger, A., Vowinckel, J., Mulleder, M., Grote, P., Capuano, F., Bluemlein, K., and Ralser, M. (2013) Tpo1-mediated spermine and spermidine export controls cell cycle delay and times antioxidant protein expression during the oxidative stress response. *EMBO Rep* **14:** 1113–1119.
Kunitomo, H., Sugimoto, A., Wilkinson, C.R., and Yamamoto, M. (1995) *Schizosaccharomyces pombe* pac2+ controls the onset of sexual development via a pathway independent of the cAMP cascade. *Curr Genet* **28:** 32–38.
Kück, U., and Böhm, J. (2013) Mating type genes and cryptic sexuality as tools for genetically manipulating industrial molds. *Appl Microbiol Biotechnol* **97:** 9609–9620.
Landt, S.G., Marinov, G.K., Kundaje, A., Kheradpour, P., Pauli, F., Batzoglou, S., *et al*. (2012) ChIP-seq guidelines and practices of the ENCODE and modENCODE consortia. *Genome Res* **22:** 1813–1831.
Langmead, B., Trapnell, C., Pop, M., and Salzberg, S.L. (2009) Ultrafast and memory-efficient alignment of short DNA sequences to the human genome. *Genome Biol* **10:** R25.
Lara-Rojas, F., Sanchez, O., Kawasaki, L., and Aguirre, J. (2011) *Aspergillus nidulans* transcription factor AtfA interacts with the MAPK SakA to regulate general stress responses, development and spore functions. *Mol Microbiol* **80:** 436–454.
Lee, S.C., Ni, M., Li, W., Shertz, C., and Heitman, J. (2010) The evolution of sex: a perspective from the fungal kingdom. *Microbiol Mol Biol Rev* **74:** 298–340.
Lee, S.H., Lee, S., Choi, D., Lee, Y.W., and Yun, S.H. (2006) Identification of the down-regulated genes in a *mat1-2*-deleted strain of *Gibberella zeae*, using cDNA subtraction and microarray analysis. *Fungal Genet Biol* **43:** 295–310.
Li, H., Handsaker, B., Wysoker, A., Fennell, T., Ruan, J., Homer, N., *et al*. (2009) The sequence alignment/map format and SAMtools. *Bioinformatics* **25:** 2078–2079.
Magnúsdóttir, E., Dietmann, S., Murakami, K., Günesdogan, U., Tang, F.C., Bao, S.Q., *et al*. (2013) A tripartite transcription factor network regulates primordial germ cell specification in mice. *Nat Cell Biol* **15:** 905–U322.
Martin, T., Lu, S.W., van Tilbeurgh, H., Ripoll, D.R., Dixelius, C., Turgeon, B.G., and Debuchy, R. (2010) Tracing the origin of the fungal alpha 1 domain places its ancestor in the HMG-box superfamily: implication for fungal mating-type evolution. *PLoS ONE* **5:** e15199.
Maruyama, M., Ichisaka, T., Nakagawa, M., and Yamanaka, S. (2005) Differential roles for Sox15 and Sox2 in transcriptional control in mouse embryonic stem cells. *J Biol Chem* **280:** 24371–24379.
Mead, J., Bruning, A.R., Gill, M.K., Steiner, A.M., Acton, T.B., and Vershon, A.K. (2002) Interactions of the Mcm1 MADS box protein with cofactors that regulate mating in yeast. *Mol Cell Biol* **22:** 4607–4621.
Mead, M.E., Stanton, B.C., Kruzel, E.K., and Hull, C.M. (2015) Targets of the Sex Inducer homeodomain proteins are required for fungal development and virulence in *Cryptococcus neoformans*. *Mol Microbiol* **95:** 804–818.
Mertin, S., McDowall, S.G., and Harley, V.R. (1999) The DNA-binding specificity of SOX9 and other SOX proteins. *Nucleic Acids Res* **27:** 1359–1364.
Metzenberg, R.L., and Glass, N.L. (1990) Mating type and mating strategies in *Neurospora*. *Bioessays* **12:** 53–59.
Miroux, B., and Walker, J.E. (1996) Over-production of proteins in *Escherichia coli*: mutant hosts that allow synthesis of some membrane proteins and globular proteins at high levels. *J Mol Biol* **260:** 289–298.
Morita, T., Yamada, T., Yamada, S., Matsumoto, K., and Ohta, K. (2011) Fission yeast ATF/CREB family protein Atf21 plays important roles in production of normal spores. *Genes Cells* **16:** 217–230.
Myers, K.S., Yan, H., Ong, I.M., Chung, D., Liang, K., Tran, F., *et al*. (2013) Genome-scale analysis of *Escherichia coli* FNR reveals complex features of transcription factor binding. *PLoS Genet* **9:** e1003565.
Nelson, B., Kurischko, C., Horecka, J., Mody, M., Nair, P., Pratt, L., *et al*. (2003) RAM: a conserved signaling network that regulates Ace2p transcription factor and polarized morphogenesis. *Mol Biol Cell* **14:** 3782–3803.

Nielsen, J. (1997) *Physiological Engineering Aspects of Penicillium chrysogenum*. Singapore: World Scientific Publishing Co. Pte. Ltd.

Paoletti, M., Seymour, F.A., Alcocer, M.J., Kaur, N., Calvo, A.M., Archer, D.B., and Dyer, P.S. (2007) Mating type and the genetic basis of self-fertility in the model fungus *Aspergillus nidulans*. *Curr Biol* **17:** 1384–1389.

Park, P.J. (2009) ChIP-seq: advantages and challenges of a maturing technology. *Nat Rev Genet* **10:** 669–680.

Penn, O., Privman, E., Ashkenazy, H., Landan, G., Graur, D., and Pupko, T. (2010) GUIDANCE: a web server for assessing alignment confidence scores. *Nucleic Acids Res* **38:** W23–W28.

Pöggeler, S., Nowrousian, M., Ringelberg, C., Loros, J.J., Dunlap, J.C., and Kück, U. (2006) Microarray and real-time PCR analyses reveal mating type-dependent gene expression in a homothallic fungus. *Mol Genet Genomics* **275:** 492–503.

Pramila, T., Miles, S., GuhaThakurta, D., Jemiolo, D., and Breeden, L.L. (2002) Conserved homeodomain proteins interact with MADS box protein Mcm1 to restrict ECB-dependent transcription to the M/G1 phase of the cell cycle. *Genes Dev* **16:** 3034–3045.

Pramila, T., Wu, W., Miles, S., Noble, W.S., and Breeden, L.L. (2006) The forkhead transcription factor Hcm1 regulates chromosome segregation genes and fills the S-phase gap in the transcriptional circuitry of the cell cycle. *Genes Dev* **20:** 2266–2278.

Rabinovich, A., Jin, V.X., Rabinovich, R., Xu, X., and Farnham, P.J. (2008) E2F *in vivo* binding specificity: comparison of consensus versus nonconsensus binding sites. *Genome Res* **18:** 1763–1777.

Robertson, G., Hirst, M., Bainbridge, M., Bilenky, M., Zhao, Y., Zeng, T., *et al*. (2007) Genome-wide profiles of STAT1 DNA association using chromatin immunoprecipitation and massively parallel sequencing. *Nat Methods* **4:** 651–657.

Ruepp, A., Zollner, A., Maier, D., Albermann, K., Hani, J., Mokrejs, M., *et al*. (2004) The FunCat, a functional annotation scheme for systematic classification of proteins from whole genomes. *Nucleic Acids Res* **32:** 5539–5545.

Schmitt, E.K., and Kück, U. (2000) The fungal CPCR1 protein, which binds specifically to beta-lactam biosynthesis genes, is related to human regulatory factor X transcription factors. *J Biol Chem* **275:** 9348–9357.

Schmitt, E.K., Bunse, A., Janus, D., Hoff, B., Friedlin, E., Kürnsteiner, H., and Kück, U. (2004) Winged helix transcription factor CPCR1 is involved in regulation of beta-lactam biosynthesis in the fungus *Acremonium chrysogenum*. *Eukaryot Cell* **3:** 121–134.

Schönig, B., Brown, D.W., Oeser, B., and Tudzynski, B. (2008) Cross-species hybridization with *Fusarium verticillioides* microarrays reveals new insights into *Fusarium fujikuroi* nitrogen regulation and the role of AreA and NMR. *Eukaryot Cell* **7:** 1831–1846.

Schrettl, M., and Haas, H. (2011) Iron homeostasis – Achilles' heel of *Aspergillus fumigatus*? *Curr Opin Microbiol* **14:** 400–405.

Schrettl, M., Bignell, E., Kragl, C., Joechl, C., Rogers, T., Arst, H., *et al*. (2004) Siderophore biosynthesis but not reductive iron assimilation is essential for *Aspergillus fumigatus* virulence. *J Exp Med* **200:** 1213–1219.

Schrettl, M., Bignell, E., Kragl, C., Sabiha, Y., Loss, O., Eisendle, M., *et al*. (2007) Distinct roles for intra- and extracellular siderophores during *Aspergillus fumigatus* infection. *PLoS Pathog* **3:** 1195–1207.

Slaven, J.W., Anderson, M.J., Sanglard, D., Dixon, G.K., Bille, J., Roberts, I.S., and Denning, D.W. (2002) Increased expression of a novel *Aspergillus fumigatus* ABC transporter gene, *atrF*, in the presence of itraconazole in an itraconazole resistant clinical isolate. *Fungal Genet Biol* **36:** 199–206.

Smith, K.M., Sancar, G., Dekhang, R., Sullivan, C.M., Li, S.J., Tag, A.G., *et al*. (2010) Transcription factors in light and circadian clock signaling networks revealed by genomewide mapping of direct targets for *Neurospora* white collar complex. *Eukaryot Cell* **9:** 1549–1556.

Smith, K.M., Phatale, P.A., Sullivan, C.M., Pomraning, K.R., and Freitag, M. (2011) Heterochromatin is required for normal distribution of *Neurospora crassa* CenH3. *Mol Cell Biol* **31:** 2528–2542.

Specht, T., Dahlmann, T.A., Zadra, I., Kürnsteiner, H., and Kück, U. (2014) Complete sequencing and chromosome-scale genome assembly of the industrial progenitor strain P2niaD18 from the penicillin producer *Penicillium chrysogenum*. *Genome Announc* **2:** e00577-14.

Spitz, F., and Furlong, E.E. (2012) Transcription factors: from enhancer binding to developmental control. *Nat Rev Genet* **13:** 613–626.

Stringer, M.A., and Timberlake, W.E. (1995) *DewA* encodes a fungal hydrophobin component of the *Aspergillus* spore wall. *Mol Microbiol* **16:** 33–44.

Tamaru, H., Zhang, X., McMillen, D., Singh, P.B., Nakayama, J., Grewal, S.I., *et al*. (2003) Trimethylated lysine 9 of histone H3 is a mark for DNA methylation in *Neurospora crassa*. *Nat Genet* **34:** 75–79.

Thorvaldsdóttir, H., Robinson, J.T., and Mesirov, J.P. (2012) Integrative Genomics Viewer (IGV): high-performance genomics data visualization and exploration. *Brief Bioinform* **14:** 178–192.

Thön, M., Al-Abdallah, Q., Hortschansky, P., and Brakhage, A.A. (2007) The thioredoxin system of the filamentous fungus *Aspergillus nidulans*: impact on development and oxidative stress response. *J Biol Chem* **282:** 27259–27269.

Todeschini, A.L., Georges, A., and Veitia, R.A. (2014) Transcription factors: specific DNA binding and specific gene regulation. *Trends Genet* **30:** 211–219.

Tsong, A.E., Miller, M.G., Raisner, R.M., and Johnson, A.D. (2003) Evolution of a combinatorial transcriptional circuit: a case study in yeasts. *Cell* **115:** 389–399.

Tuch, B.B., Galgoczy, D.J., Hernday, A.D., Li, H., and Johnson, A.D. (2008) The evolution of combinatorial gene regulation in fungi. *PLoS Biol* **6:** e38.

Turgeon, B.G., and Yoder, O.C. (2000) Proposed nomenclature for mating type genes of filamentous ascomycetes. *Fungal Genet Biol* **31:** 1–5.

Valouev, A., Johnson, D.S., Sundquist, A., Medina, C., Anton, E., Batzoglou, S., *et al*. (2008) Genome-wide analysis of transcription factor binding sites based on ChIP-Seq data. *Nat Methods* **5:** 829–834.

Wada, R., Maruyama, J., Yamaguchi, H., Yamamoto, N., Wagu, Y., Paoletti, M., *et al*. (2012) Presence and

functionality of mating type genes in the supposedly asexual filamentous fungus *Aspergillus oryzae*. *Appl Environ Microbiol* **78:** 2819–2829.
Wang, Z., Lopez-Giraldez, F., Lehr, N., Farré, M., Common, R., Trail, F., and Townsend, J.P. (2014) Global gene expression and focused knockout analysis reveals genes associated with fungal fruiting body development in *Neurospora crassa*. *Eukaryot Cell* **13:** 154–169.
Wasserstrom, L., Lengeler, K.B., Walther, A., and Wendland, J. (2013) Molecular determinants of sporulation in *Ashbya gossypii*. *Genetics* **195:** 87–99.
Waterhouse, A.M., Procter, J.B., Martin, D.M., Clamp, M., and Barton, G.J. (2009) Jalview Version 2-a multiple sequence alignment editor and analysis workbench. *Bioinformatics* **25:** 1189–1191.
Wettenhall, J.M., Simpson, K.M., Satterley, K., and Smyth, G.K. (2006) affylmGUI: a graphical user interface for linear modeling of single channel microarray data. *Bioinformatics* **22:** 897–899.
Wiemann, P., Brown, D.W., Kleigrewe, K., Bok, J.W., Keller, N.P., Humpf, H.U., and Tudzynski, B. (2010) FfVel1 and FfLae1, components of a velvet-like complex in *Fusarium fujikuroi*, affect differentiation, secondary metabolism and virulence. *Mol Microbiol* **77:** 972–994.
Wolfers, S., Kamerewerd, J., Nowrousian, M., Sigl, C., Zadra, I., Kürnsteiner, H., *et al*. (2014) Microarray hybridization analysis of light-dependent gene expression in *Penicillium chrysogenum* identifies bZIP transcription factor PcAtfA. *J Basic Microbiol* **54:** 1–10.
Wong, K.H., Hynes, M.J., Todd, R.B., and Davis, M.A. (2007) Transcriptional control of *nmrA* by the bZIP transcription factor MeaB reveals a new level of nitrogen regulation in *Aspergillus nidulans*. *Mol Microbiol* **66:** 534–551.
Wunderlich, Z., and Mirny, L.A. (2009) Different gene regulation strategies revealed by analysis of binding motifs. *Trends Genet* **25:** 434–440.
Zaret, K.S., and Carroll, J.S. (2011) Pioneer transcription factors: establishing competence for gene expression. *Genes Dev* **25:** 2227–2241.

Supporting information

Additional supporting information may be found in the online version of this article at the publisher's web-site.